REVISTA MATEMÁTICA COMPLUTENSE
Volumen 12, número 1: 1999

Hyperbolic systems of conservation laws.

Alberto BRESSAN

Abstract

This is a survey paper, written in the occasion of an invited talk given by the author at the Universidad Complutense in Madrid, October 1998. Its purpose is to provide an account of some recent advances in the mathematical theory of hyperbolic systems of conservation laws in one space dimension. After a brief review of basic concepts, we describe in detail the method of wave-front tracking approximation and present some of the latest results on uniqueness and stability of entropy weak solutions.

1 Review of basic theory

This chapter reviews the basic definitions and properties of systems of conservation laws. For a comprehensive introduction to the theory of hyperbolic systems we refer to [22, 23, 24].

1.1 Basic definitions

A single conservation law in one space dimension is a first order partial differential equation of the form

$$u_t + f(u)_x = 0. \tag{1.1}$$

Here u is the *conserved quantity* while f is the *flux*. Integrating (1.1) over the interval $[a, b]$ one obtains

---

AMS Subject Classification: 35L65.
Servicio Publicaciones Univ. Complutense. Madrid, 1999.

$$\begin{aligned} \frac{d}{dt}\int_a^b u(t,x)\,dx &= \int_a^b u_t(t,x)\,dx \\ &= -\int_a^b f(u(t,x))_x\,dx \\ &= f(u(t,a)) - f(u(t,b)) \\ &= \text{[inflow at } a\text{]} - \text{[outflow at } b\text{]} \end{aligned} \tag{1.2}$$

In other words, the quantity u is neither created nor destroyed: the total amount of u contained inside any given interval $[a,b]$ can change only due to flow of u across the two endpoints.

Using the chain rule, (1.1) can be written in the quasilinear form

$$u_t + a(u)u_x = 0, \tag{1.3}$$

where $a = f'$ is the derivative of f. For smooth solutions, the two equations (1.1) and (1.3) are entirely equivalent. If u has a jump, however, the left hand side of (1.3) will contain the product of a discontinuous function $a(u)$ with the distributional derivative u_x, which in this case contains a Dirac mass at the point of jump. In general, such a product is not well defined. Hence (1.3) is meaningful only within a class of continuous functions. On the other hand, working with the equation in divergence form (1.1) allows us to consider discontinuous solutions as well, interpreted in distributional sense. More precisely, a locally integrable function $u = u(t,x)$ is a *weak solution* of (1.1) provided that

$$\iint [u\phi_t + f(u)\phi_x]\,dxdt \;=\; 0 \tag{1.4}$$

for every differentiable function with compact support $\phi \in C_c^1$.

The main object of our study will be the $n \times n$ *system of conservation laws*

$$\begin{cases} \frac{\partial}{\partial t}u_1 + \frac{\partial}{\partial x}[\quad f_1(u_1,\ldots,u_n)] = 0, \\ \qquad\qquad \cdots \\ \frac{\partial}{\partial t}u_n + \frac{\partial}{\partial x}[\quad f_n(u_1,\ldots,u_n)] = 0. \end{cases} \tag{1.5}$$

For simplicity, this will still be written in the form (1.1), but keeping in mind that now $u = (u_1,\ldots,u_n)$ is a vector in $\mathbb{R}^n$ and that $f = (f_1,\ldots,f_n)$ is a map from $\mathbb{R}^n$ into itself. Calling $A(u) \doteq Df(u)$ the

$n \times n$ Jacobian matrix of the map f at the point u, the system (1.5) can be written in the quasilinear form

$$u_t + A(u)u_x = 0. \tag{1.6}$$

We say that the above system is *strictly hyperbolic* if every matrix $A(u)$ has n real, distinct eigenvalues, say $\lambda_1(u) < \cdots < \lambda_n(u)$. In this case, one can find dual bases of left and right eigenvectors of $A(u)$, denoted by $l_1(u), \ldots, l_n(u)$ and $r_1(u), \ldots, r_n(u)$, with

$$l_i(u) \cdot r_j(u) = \begin{cases} 1 & \text{if } i = j, \\ 0 & \text{if } i \neq j. \end{cases}$$

1.2 Linear systems

We consider here two elementary cases where the solution of the Cauchy problem can be written explicitly.

The linear homogeneous scalar Cauchy problem with constant coefficients has the form

$$u_t + \lambda u_x = 0, \qquad u(0,x) = \bar{u}(x), \tag{1.7}$$

with $\lambda \in \mathbb{R}$. If $\bar{u} \in \mathcal{C}^1$, one easily checks that the travelling wave

$$u(t,x) = \bar{u}(x - \lambda t) \tag{1.8}$$

provides a classical solution to (1.7). In the case where the initial condition $\bar{u}$ is not differentiable and we only have $\bar{u} \in \mathbf{L}^1_{loc}$, the function u defined by (1.8) can still be interpreted as a solution, in distributional sense.

Next, consider the homogeneous system with constant coefficients

$$u_t + Au_x = 0, \qquad u(0,x) = \bar{u}(x), \tag{1.9}$$

where A is a $n \times n$ hyperbolic matrix, with real eigenvalues $\lambda_1 < \cdots < \lambda_n$ and eigenvectors r_i, l_i, chosen so that $l_i \cdot r_j = \delta_{ij}$. Call $u_i \doteq l_i \cdot u$ the coordinates of a vector $u \in \mathbb{R}^n$ w.r.t. the basis of right eigenvectors $\{r_1, \cdots, r_n\}$. Multiplying (1.9) on the left by $l_1, \ldots, l_n$ we obtain

$$(u_i)_t + \lambda_i (u_i)_x = (l_i u)_t + \lambda_i (l_i u)_x = l_i u_t + l_i A u_x = 0,$$

$$u_i(0,x) = l_i\bar{u}(x) \doteq \bar{u}_i(x).$$

Therefore, (1.9) decouples into n scalar Cauchy problems, which can be solved separately in the same way as (1.7). The function

$$u(t,x) = \sum_{i=1}^{n} \bar{u}_i(x-\lambda_i t)\, r_i \tag{1.10}$$

now provides a solution to (1.9), because

$$u_t(t,x) = \sum_{i=1}^{n} -\lambda_i(l_i \cdot \bar{u}_x(x-\lambda_i t))r_i = -Au_x(t,x).$$

Observe that in the scalar case (1.7) the initial profile is shifted with constant speed λ. For the system (1.9), the initial profile is decomposed as a sum of n waves, each travelling with one of the characteristic speeds $\lambda_1, \ldots, \lambda_n$.

As a special case, consider the Riemann initial data

$$\bar{u}(x) = \begin{cases} u^- & \text{if } x < 0, \\ u^+ & \text{if } x > 0. \end{cases}$$

The corresponding solution (1.10) can then be obtained as follows.

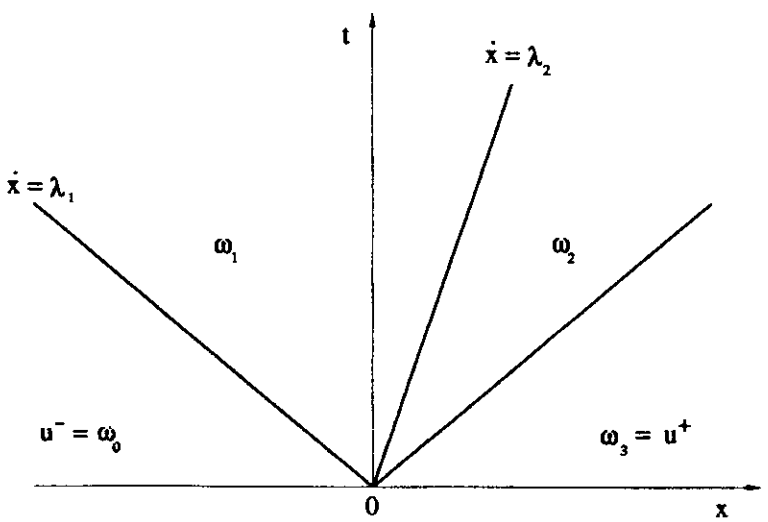

figure 1

Write the vector $u^+ - u^-$ as a linear combination of eigenvectors of A, i.e.

$$u^+ - u^- = \sum_{j=1}^{n} c_j r_j.$$

Define the intermediate states

$$\omega_i \doteq u^- + \sum_{j \le i} c_j r_j, \qquad i = 0, \dots, n,$$

so that each difference $\omega_i - \omega_{i-1}$ is an i-eigenvector of A. The solution then takes the form (fig. 1):

$$u(t,x) = \begin{cases} \omega_0 = u^- & \text{for } x/t < \lambda_1, \\ \dots & \\ \omega_i & \text{for } \lambda_i < x/t < \lambda_{i+1}, \\ \dots & \\ \omega_n = u^+ & \text{for } x/t > \lambda_n. \end{cases} \tag{1.11}$$

1.3 Loss of regularity

A basic feature of nonlinear systems of the form (1.1) is that, even for smooth initial data, the solution of the Cauchy problem may develop discontinuities in finite time [16]. To achieve a global existence result, it is thus essential to work within a class of discontinuous functions, interpreting the equations (1.1) in their distributional sense (1.4).

Example 1. Consider the scalar conservation law (inviscid Burgers' equation)

$$u_t + \left(\frac{u^2}{2}\right)_x = 0 \tag{1.12}$$

with initial condition

$$u(0,x) = \bar{u}(x) = \frac{1}{1+x^2}.$$

For $t > 0$ small the solution can be found by the method of characteristics. Indeed, if u is smooth, (1.12) is equivalent to

$$u_t + u u_x = 0. \tag{1.13}$$

By (1.13) the directional derivative of the function $u = u(t,x)$ along the vector $(1,u)$ vanishes. Therefore, u must be constant along the characteristic lines in the t-x plane:

$$t \mapsto (t,\ x+tu) = \left(t,\ x+\frac{t}{1+x^2}\right).$$

For $t < T \doteq 8/\sqrt{27}$, these lines do not intersect (fig. 2). The solution to our Cauchy problem is thus given implicitly by

$$u\left(t,\ x+\frac{t}{1+x^2}\right) = \frac{1}{1+x^2}\,. \tag{1.14}$$

On the other hand, when $t > 8/\sqrt{27}$, the characteristic lines start to intersect. As a result, the map

$$x \mapsto x+\frac{t}{1+x^2}$$

is not one-to-one and (1.14) no longer defines a single valued solution of our Cauchy problem.

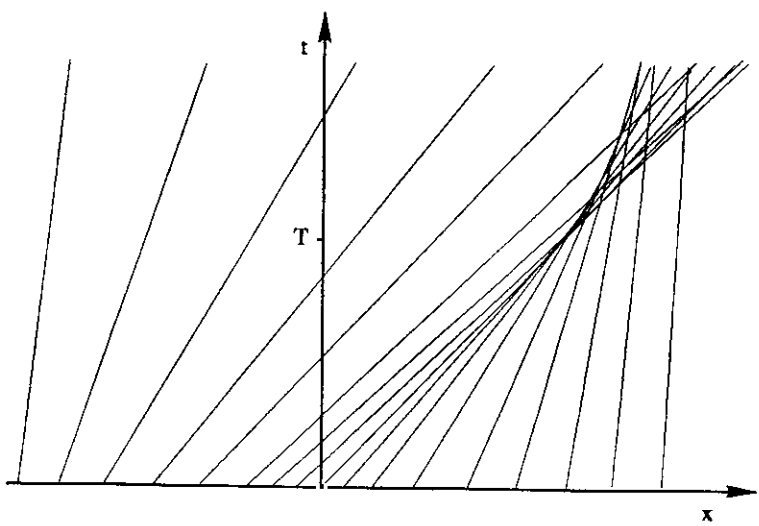

figure 2

An alternative point of view is the following (fig. 3). As time increases, points on the graph of $u(t,\cdot)$ move horizontally with speed u,

equal to their distance from the x-axis. This determines a change in the profile of the solution. As t approaches the critical time $T \doteq 8/\sqrt{27}$, one has

$$\lim_{t \to T-} \left\{ \inf_{x \in \mathbb{R}} u_x(t,x) \right\} = -\infty,$$

and no classical solution exists beyond time T. The solution can be prolonged for all times $t \geq 0$ only within a class discontinuous functions.

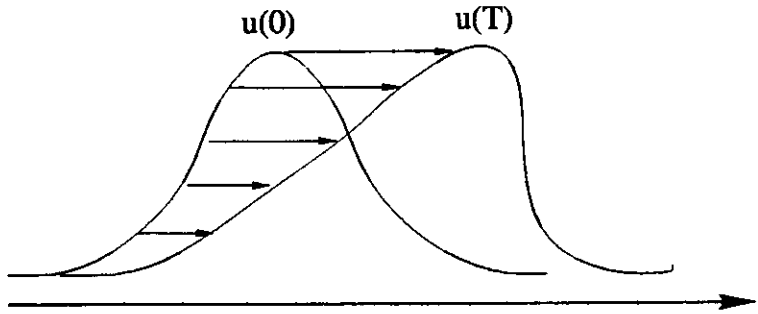

figure 3

1.4 Discontinuous solutions

Motivated by the previous example, for a nonlinear system of conservation laws, global solutions must be studied in a space of discontinuous functions. We now derive conditions imposed by (1.4) on a solution at points of jump. To fix the ideas, consider a piecewise smooth solution $u = u(t,x)$ having a discontinuity across a line $x = \gamma(t)$. Call

$$u^{\pm}(t) = \lim_{x \to \gamma(t)\pm} u(t,x)$$

the right and left limits of $u(t,\cdot)$ at the point of jump. For any $\phi \in \mathcal{C}_c^1$, applying the divergence theorem to the vector field $(u \cdot \phi,\ f(u) \cdot \phi)$ on the two domains on the right and on the left of γ we obtain

$$\begin{aligned} \iint \{u \cdot \phi_t + f(u) \cdot \phi_x\}\, dxdt &= -\iint \{u_t + A(u)u_x\} \cdot \phi \, dxdt \\ &+ \int \Big\{ [u^+(t) - u^-(t)]\dot{\gamma}(t) - [f(u^+(t)) - f(u^-(t))] \Big\} \cdot \phi(t,\ \gamma(t))\, dt. \end{aligned} \tag{1.15}$$

Since (1.15) is valid for every differentiable ϕ with compact support, from (1.4) it follows that the equation (1.6) must hold at all points outside

the line of jump. Moreover, along γ one must have

$$[u^+ - u^-]\dot{\gamma} = f(u^+) - f(u^-), \tag{1.16}$$

The vector equations (1.16) are the famous *Rankine-Hugoniot conditions*. They form a set of n scalar equations relating the right and left states $u^+, u^- \in \mathbb{R}^n$ and the speed $\dot{\gamma}$ of the shock.
Define the averaged matrix

$$A(u,v) \doteq \int_0^1 A(\theta u + (1-\theta)v)\, d\theta \tag{1.17}$$

with $A = Df$ the Jacobian matrix of f, and call $\lambda_i(u,v)$ its eigenvalues. One can then write (1.16) in the equivalent form

$$\begin{aligned} \dot{\gamma}\cdot(u^+ - u^-) &= f(u^+) - f(u^-) \\ &= D\int_0^1 Df(\theta u^+ + (1-\theta)u^-)\cdot(u^+ - u^-)\, d\theta \\ &= A(u^+, u^-)\cdot(u^+ - u^-). \end{aligned} \tag{1.18}$$

In other words, the Rankine-Hugoniot equations hold iff the jump $u^+ - u^-$ is an eigenvector of the averaged matrix $A(u^+, u^-)$ and the speed $\dot{\gamma}$ coincides with the corresponding eigenvalue.

In the scalar case, (1.16) reduces to a single equation. One can thus assign u^+, u^- arbitrarily and use the equation to determine the shock speed:

$$\dot{\gamma} = \frac{f(u^+) - f(u^-)}{u^+ - u^-} = \frac{1}{u^+ - u^-}\int_{u^-}^{u^+} f'(u)\, du. \tag{1.19}$$

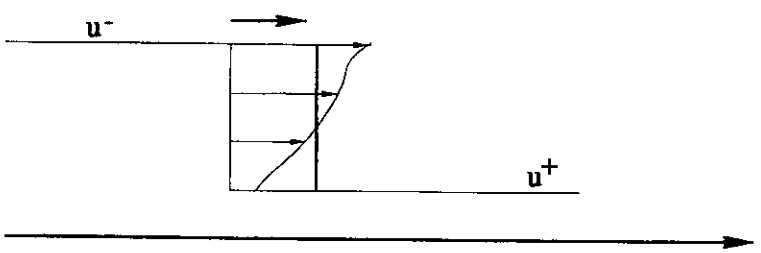

figure 4

The last expression in (1.19) shows that the shock speed coincides with the average of the characteristic speeds $f'(u)$ over the interval

$[u^-, u^+]$. Of course (fig. 4), this is closely connected with the conservation of the total area below the graph of $u(t, \cdot)$.

Example 2. In the case of Burger's equation $u_t + (u^2/2)_x = 0$, one finds

$$\dot{\gamma} = \frac{[(u^+)^2/2] - [(u^-)^2/2]}{u^+ - u^-} = \frac{u^+ + u^-}{2}. \tag{1.20}$$

1.5 Entropy conditions

In the presence of discontinuities, the Rankine-Hugoniot equations (1.16) may not suffice to single out a unique solution to the Cauchy problem.

Example 3. For Burgers' equation (1.12), the Cauchy problem with initial data

$$u(0, x) = \begin{cases} 1 & \text{if} \quad x \geq 0, \\ 0 & \text{if} \quad x < 0, \end{cases}$$

admits infinitely many weak solutions. Namely, for every $\alpha \in [0, 1]$, the piecewise constant function

$$u_\alpha(t, x) = \begin{cases} 0 & \text{if} \quad x < \alpha t/2, \\ \alpha & \text{if} \quad \alpha t/2 \leq x < (1+\alpha)t/2, \\ 1 & \text{if} \quad x \geq (1+\alpha)t/2, \end{cases}$$

provides a solution in distribution sense. Indeed, the Rankine-Hugoniot conditions (1.20) hold along the two lines of discontinuity $\xi_1(t) = \alpha t/2$, $\xi_2(t) = (\alpha + 1)t/2$. Outside these two lines, u_α is constant, hence the equation $u_t + uu_x = 0$ is trivially satisfied.

From the previous example it is clear that, in order to achieve a theorem stating uniqueness and continuous dependence on the initial data, the notion of weak solution must be supplemented with further "admissibility conditions", possibly motivated by physical considerations. Some of these conditions will be presently discussed.

Admissibility Condition 1 (Vanishing viscosity). A weak solution u of (1.1) is admissible if there exists a sequence of smooth solutions u^ε to

$$u_t^\varepsilon + A(u^\varepsilon)u_x^\varepsilon = \varepsilon u_{xx}^\varepsilon \tag{1.21}$$

which converge to u in $\mathbf{L}^1$ as $\varepsilon \to 0+$.

Unfortunately, it is very difficult to provide uniform estimates on solutions to the parabolic system (1.21) and to characterize the corresponding limits as $\varepsilon \to 0+$. From the above condition, however, one can deduce other conditions which can be more easily verified in practice.

A continuously differentiable function $\eta : \mathbb{R}^n \mapsto \mathbb{R}$ is called an *entropy* for the system (1.1), with *entropy flux* $q : \mathbb{R}^n \mapsto \mathbb{R}$ if

$$D\eta(u) \cdot Df(u) = Dq(u) \qquad u \in \mathbb{R}^n. \tag{1.22}$$

Observe that (1.22) implies that, if $u = u(t,x)$ is a $\mathcal{C}^1$ solution of (1.1), then

$$[\eta(u)]_t + [q(u)]_x = 0. \tag{1.23}$$

Indeed,

$$D\eta(u)u_t + Dq(u)u_x = D\eta(u)[-Df(u)u_x] + Dq(u)u_x = 0.$$

Hence, whenever we have a smooth solution of (1.1), not only the quantities $u_1, \ldots, u_n$ are conserved, but the additional conservation law (1.23) holds as well. On the other hand, when u is discontinuous, in general it does not provide a weak solution to (1.23), i.e. $\eta = \eta(u)$ is not a conserved quantity. This can be seen in Example 2, taking $\eta(u) = u^3$ and $q(u) = (3/4)u^4$.

We now study how a convex entropy behaves in the presence of a small diffusion term. Assume $\eta, q \in \mathcal{C}^2$, with η convex. Multiplying both sides of (1.21) on the left by $D\eta(u^\varepsilon)$ one finds

$$[\eta(u^\varepsilon)]_t + [q(u^\varepsilon)]_x = \varepsilon D\eta(u^\varepsilon)u^\varepsilon_{xx} = \varepsilon\{[\eta(u^\varepsilon)]_{xx} - D^2\eta(u^\varepsilon)\cdot(u^\varepsilon_x \otimes u^\varepsilon_x)\}. \tag{1.24}$$

Observe that the last term in (1.24) satisfies

$$D^2\eta(u^\varepsilon)(u^\varepsilon_x \otimes u^\varepsilon_x) = \sum_{i,j=1}^{n} \frac{\partial^2\eta(u^\varepsilon)}{\partial u_i \partial u_j} \cdot \frac{\partial u_i^\varepsilon}{\partial x}\frac{\partial u_j^\varepsilon}{\partial x} \geq 0,$$

because η is convex, hence its second derivative at any point u^ε is a positive semidefinite quadratic form. Multiplying (1.24) by a nonnegative smooth function φ with compact support and integrating by parts, we thus have

$$\iint \{\eta(u^\varepsilon)\varphi_t + q(u^\varepsilon)\varphi_x\}\, dxdt \geq -\varepsilon \iint \eta(u^\varepsilon)\varphi_{xx}\, dxdt.$$

If $u^\varepsilon \to u$ in $\mathbf{L}^1$ as $\varepsilon \to 0$, the previous inequality yields

$$\iint \{\eta(u)\varphi_t + q(u)\varphi_x\}\, dxdt \geq 0 \tag{1.25}$$

whenever $\varphi \in C_c^1$, $\varphi \geq 0$. The above can be restated by saying that $\eta(u)_t + q(u)_x \leq 0$ in distribution sense, i.e. any convex entropy does not increase in time. The previous analysis leads to:

Admissibility Condition 2 (Entropy inequality). A weak solution u of (1.1) is *entropy-admissible* if

$$[\eta(u)]_t + [q(u)]_x \leq 0 \tag{1.26}$$

in the sense of distributions, for every pair (η, q), where η is a convex entropy for (1.1) and q is the corresponding entropy flux.

Let $u = u(t,x)$ be a piecewise smooth function with jumps along the lines $x = x_\alpha(t)$, $\alpha = 1, , m$. Repeating the computations at (1.15), one finds that u satisfies (1.26) provided that

$$D\eta(u)u_t + Dq(u)u_x \leq 0$$

outside the jumps, while

$$\dot{x}_\alpha\Big[\eta(u(x_\alpha+)) - \eta(u(x_\alpha-))\Big] \geq q(u(x_\alpha+)) - q(u(x_\alpha-)) \tag{1.27}$$

along each shock line.

Of course, the above admissibility condition can be useful only if some nontrivial convex entropy for the system (1.1) is known. For $n \times n$ systems, (1.22) can be regarded as a first order system of n equations for the two scalar variables η, q. When $n \geq 3$, this system is overdetermined. In general, one should thus expect to find solutions only in the case $n \leq 2$. However, there are important physical examples of larger systems which admit a nontrivial entropy function.

In the scalar case, convex entropy functions are easy to construct. In particular, for each $k \in \mathbb{R}$, consider the functions

$$\eta(u) = |u - k|, \qquad q(u) = \operatorname{sgn}(u-k)\cdot(f(u) - f(k)).$$

It is easily checked that η, q are locally Lipschitz continuous and satisfy (1.22) at every $u \neq k$. Although $\eta, q \notin \mathcal{C}^1$, we can still regard η as a convex entropy for (1.1), with entropy flux q. Following Kruzhkov [17], we say that a bounded measurable function u is an *entropic solution* of (1.1) if

$$\iint \Big\{ |u-k|\varphi_t + \mathrm{sgn}(u-k)(f(u)-f(k))\varphi_x \Big\}\, dxdt \geq 0 \tag{1.28}$$

for every constant $k \in \mathbb{R}$ and every $\mathcal{C}^1$ function $\varphi \geq 0$ with compact support.

According to (1.28), one can show that a shock connecting the left and right states u^-, u^+ is admissible if and only if

$$\frac{f(u^+)-f(u^*)}{u^+-u^*} \leq \frac{f(u^*)-f(u^-)}{u^*-u^-} \tag{1.29}$$

for every $u^* = \alpha u^+ + (1-\alpha)u^-$, with $0 < \alpha < 1$. The above inequality can be interpreted as a stability condition. Indeed, let $u^* \in [u^-, u^+]$ be an intermediate state and consider a slightly perturbed solution (fig. 5a-b), where the shock (u^-, u^+) is decomposed as two separate jumps, (u^-, u^*) and (u^*, u^+), say located at $\gamma^-(t) < \gamma^+(t)$ respectively. By the the Rankine-Hugoniot conditions, the two sides of (1.29) yield precisely the speeds of these jumps. If the inequality holds, then $\dot\gamma^- \geq \dot\gamma^+$, so that the backward shock travels at least as fast as the forward one. Therefore, the two shocks will not split apart as time increases, and the perturbed solution will remain close to the original solution possessing a single shock.

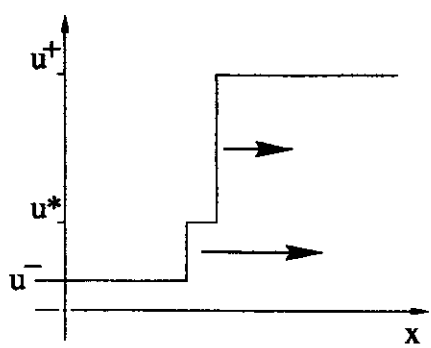

figure 5a

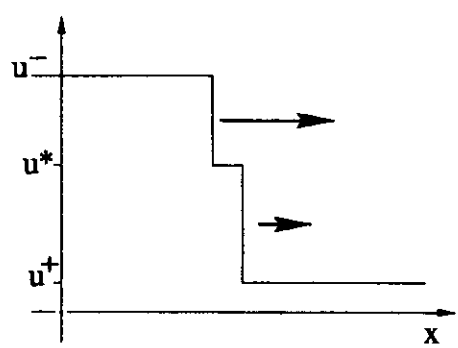

figure 5b

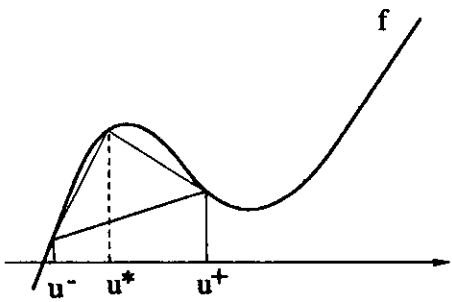

figure 6a

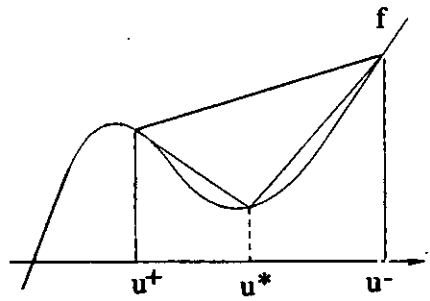

figure 6b

Observing that the Rankine-Hugoniot speed of a shock in (1.19) is given by the slope of the secant line to the graph of f through the points u^-, u^+, the condition (1.29) holds if and only if for every $\alpha \in [0,1]$ one has

$$\begin{cases} f(\alpha u^+ + (1-\alpha)u^-) \geq \alpha f(u^+) + (1-\alpha) f(u^-) & \text{if} \quad u^- < u^+, \\ f(\alpha u^+ + (1-\alpha)u^-) \leq \alpha f(u^+) + (1-\alpha) f(u^-) & \text{if} \quad u^- > u^+. \end{cases} \tag{1.30}$$

In other words, when $u^- < u^+$ the graph of f should remain above the secant line (fig.6a). When $u^- > u^+$, the graph of f should remain below the secant line (fig.6b).

A third admissibility condition, due to Lax [18], is particularly useful because it can be applied to any system and has a very intuitive geometrical meaning. According to (1.18), every shock will travel with a speed $\dot{\gamma} = \lambda_i(u^-, u^+)$ equal to an eigenvalue of the averaged matrix $A(u^-, u^+)$. In this setting, the Lax condition requires that the i-characteristics, travelling on the left and on the right of the shock with speeds $\lambda_i(u^-)$, $\lambda_i(u^+)$ respectively, both run into the shock:

Admissibility Condition 3 (Lax Condition). A shock connecting the states u^-, u^+, travelling with speed $\dot{\gamma} = \lambda_i(u^-, u^+)$ is admissible if

$$\lambda_i(u^-) \geq \lambda_i(u^-, u^+) \geq \lambda_i(u^+). \tag{1.31}$$

This situation is illustrated in fig. 7a. On the other hand, one can check that for the solutions constructed in Example 3, neither of the two shocks satisfies the above condition (fig. 7b).

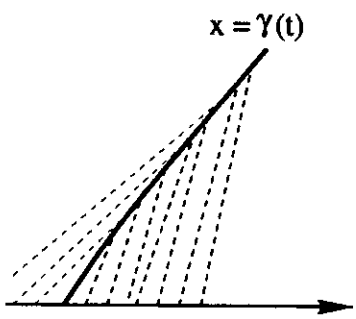

figure 7a

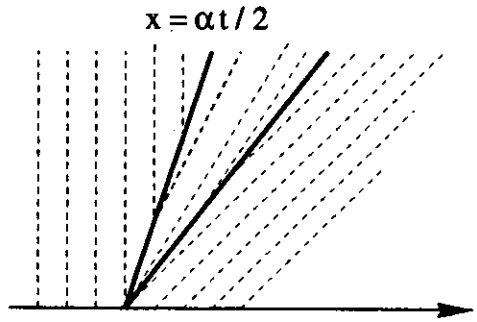

figure 7b

1.6 Shock and rarefaction curves

Fix a state $u_0 \in \mathbb{R}^n$ and an index $i \in \{1, \ldots, n\}$. As before, let $r_i(u)$ be the i-th eigenvector of the Jacobian matrix $A(u) = Df(u)$. The integral curve of the vector field r_i through the point u_0 is called the *i-rarefaction curve* through u_0. It is obtained by solving the Cauchy problem in state space:

$$\frac{du}{d\sigma} = r_i(u), \qquad u(0) = u_0. \tag{1.32}$$

We shall denote this curve as

$$\sigma \mapsto R_i(\sigma)(u_0). \tag{1.33}$$

Of course, the parametrization depends on the choice of the eigenvectors r_i. In particular, if we impose the normalization $|r_i(u)| \equiv 1$, then the rarefaction curve (1.33) will be parametrized by arc-length.

Next, for a fixed $u_0 \in \mathbb{R}^n$ and $i \in \{1, \ldots, n\}$, we consider the curve of states u which can be connected to the right of u_0 by an i-shock, satisfying the Rankine-Hugoniot equations (1.16). According to (1.18), these equations imply that the vector $u - u_0$ is a right i-eigenvector of the averaged matrix $A(u, u_0)$. By a theorem of basic linear algebra, this holds if and only if $u - u_0$ is orthogonal to every left j-eigenvector of $A(u, u_0)$, with $j \neq i$. The Rankine-Hugoniot equations can thus be written in the form

$$l_j(u, u_0) \cdot (u - u_0) = 0 \qquad \text{for all } \ j \neq i, \tag{1.34}$$

together with $\dot{\gamma} = \lambda_i(u, u_0)$. We regard (1.34) as a system of $n-1$ scalar equations in n variables (the n components of the vector u). Linearizing (1.34) at the point $u = u_0$ we obtain the linear system

$$l_j(u_0) \cdot (w - u_0) = 0 \qquad j \neq i,$$

whose solutions are all the points $w = u_0 + cr_i(u_0)$, $c \in \mathbb{R}$. By the implicit function theorem, it thus follows that the set of solutions is a regular curve, tangent to the vector r_i at the point u_0. This will be called the *shock curve* through the point u_0 and denoted as

$$\sigma \mapsto S_i(\sigma)(u_0). \tag{1.35}$$

Using a suitable parametrization, the two curves R_i, S_i will have a second order contact at the point u_0 (fig. 8). More precisely, the following estimates hold [18, 24].

$$\begin{cases} R_i(\sigma)(u_0) &= u_0 + \sigma r_i(u_0) + \mathcal{O}(1) \cdot \sigma^2, \\ S_i(\sigma)(u_0) &= u_0 + \sigma r_i(u_0) + \mathcal{O}(1) \cdot \sigma^2, \end{cases} \tag{1.36}$$

$$|R_i(\sigma)(u_0) - S_i(\sigma)(u_0)| = \mathcal{O}(1) \cdot \sigma^3, \tag{1.37}$$

$$\lambda_i(S_i(\sigma)(u_0),\ u_0) = \lambda_i(u_0) + \frac{\sigma}{2}(D\lambda_i(u_0)) \cdot r_i(u_0) + \mathcal{O}(1) \cdot \sigma^2. \tag{1.38}$$

Here and throughout the following, the Landau symbol $\mathcal{O}(1)$ denotes a quantity whose absolute value satisfies a uniform bound, depending only on the system (1.1).

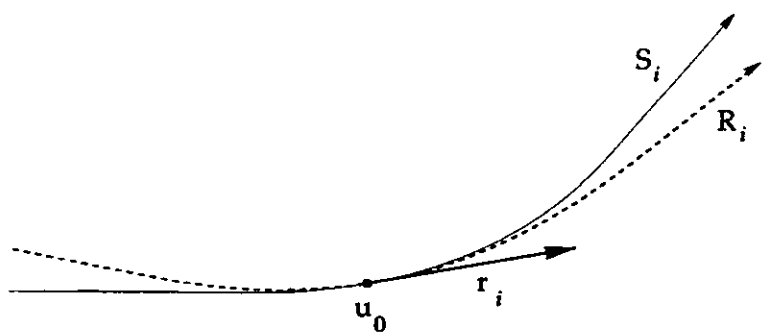

figure 8

1.7 The Riemann problem

The basic building block toward the solution of the general Cauchy problem for (1.1) is the the solution of the following initial value problem:

$$u_t + f(u)_x = 0, \qquad u(0,x) = \begin{cases} u^- & \text{if} \quad x < 0, \\ u^+ & \text{if} \quad x > 0. \end{cases} \tag{1.39}$$

The initial data have here a very simple form, being constant for $x < 0$ and for $x > 0$, with a single jump at the origin.

Before describing the general solution of (1.39), a key assumption will be introduced. Recall that $\lambda_i(u)$, $r_i(u)$ denote the i-th eigenvalue and right eigenvector of the matrix $A(u) = Df(u)$. Following [18], the i-th characteristic field is called *genuinely nonlinear* if $D\lambda_i(u) \cdot r_i(u) \neq 0$ for all u. On the other hand, if $D\lambda_i(u) \cdot r_i(u) = 0$ for all u, we say that the i-th field is *linearly degenerate*. In the genuinely nonlinear case, we can choose the orientation of the eigenvectors r_i so that

$$D\lambda_i(u) \cdot r_i(u) > 0. \tag{1.40}$$

Observe that if the i-th characteristic field is genuinely nonlinear, then the characteristic speed λ_i is monotonically increasing along the i-rarefaction curves (1.33). On the other hand, if the i-th field is linearly degenerate, then λ_i is constant along the curves R_i. Throughout the following, a solution of the Riemann problem will be constructed under the following assumptions:

(♣) The system (1.1) is strictly hyperbolic with smooth coefficients. For each $i \in \{1, \ldots, n\}$, the i-th characteristic field is either genuinely nonlinear or linearly degenerate.

We shall first study three special cases:

1. Centered Rarefaction Waves. Let the i-th field be genuinely nonlinear, and assume that u^+ lies on the positive i-rarefaction curve through u^-, i.e. $u^+ = R_i(\sigma)(u^-)$ for some $\sigma > 0$. For each $s \in [0, \sigma]$, define

$$\lambda_i(s) = \lambda_i(R_i(s)(u^-)).$$

By genuine nonlinearity, the map $s \mapsto \lambda_i(s)$ is strictly increasing. For $t \geq 0$, the function

$$u(t,x) = \begin{cases} u^- & \text{if} \quad x < t\lambda_i(u^-), \\ R_i(s)(u^-) & \text{if} \quad x = t\lambda_i(s), \quad s \in [0,\sigma], \\ u^+ & \text{if} \quad x > t\lambda_i(u^+), \end{cases} \tag{1.41}$$

is then a piecewise smooth weak solution of the Riemann problem (1.39). Indeed,

$$\lim_{t \to 0+} \|u(t,\cdot) - \bar{u}\|_{\mathbf{L}^1} = 0.$$

Moreover, the equation (1.6) is trivially satisfied in the sectors where $x < t\lambda_i(u^-)$ or $x > t\lambda_i(u^+)$, since here $u_t = u_x = 0$. Next, assume $x = t\lambda_i(s)$ for some $s \in]0,\sigma[$. Since u is constant along each ray $\{(t',x');\ x' = t'\lambda_i(s)\}$, we clearly have

$$u_t(t,x) + \lambda_i(s)u_x(t,x) = 0. \tag{1.42}$$

Observing that

$$u_x = \frac{\partial u}{\partial x} = \frac{dR_i(s)(u^-)}{ds} \cdot \frac{ds}{d\lambda_i(s)} \cdot \frac{d\lambda_i}{dx} = r_i(u) \cdot \left(\frac{d\lambda_i(s)}{ds}\right)^{-1} \cdot \frac{1}{t}$$

is an eigenvector of the matrix $A(u)$ with eigenvalue $\lambda_i(s) = \lambda_i(u(t,x))$, from (1.42) it again follows (1.6).

Observe that the assumption $\sigma > 0$ is essential for the validity of this construction. In the opposite case $\sigma < 0$, the definition (1.41) would yield a triple-valued function in the region where $x/t \in [\lambda_i(u^+),\ \lambda_i(u^-)]$.

2. Shocks. Assume again that the i-th family is genuinely nonlinear and that the state u^+ is connected to the right of u^- by an i-shock, i.e. $u^+ = S_i(\sigma)(u^-)$. Then, calling $\lambda \doteq \lambda_i(u^+,u^-)$ the Rankine-Hugoniot speed of the shock, the function

$$u(t,x) = \begin{cases} u^- & \text{if} \quad x < \lambda t, \\ u^+ & \text{if} \quad x > \lambda t, \end{cases} \tag{1.43}$$

provides a piecewise constant solution to the Riemann problem. Observe that, if $\sigma < 0$, than this solution is entropy admissible in the sense of Lax. Indeed, since the speed is monotonically increasing along the shock curve, recalling (1.38) we have

$$\lambda_i(u^+) < \lambda_i(u^-,u^+) < \lambda_i(u^+). \tag{1.44}$$

In the case $\sigma > 0$, however, one has $\lambda_i(u^-) < \lambda_i(u^+)$ and the admissibility condition (1.31) is violated.

3. Contact discontinuities. Assume that the i-th field is linearly degenerate and that the state u^+ lies on the i-th rarefaction curve through u^-, i.e. $u^+ = R_i(\sigma)(u^-)$ for some σ. By assumption, the i-th characteristic speed λ_i is constant along this curve. Choosing $\lambda = \lambda(u^-)$, the piecewise constant function (1.43) then provides a solution to the Riemann problem (1.39). Indeed, the Rankine-Hugoniot conditions hold at the point of jump:

$$\begin{aligned} f(u^+) - f(u^-) &= \int_0^\sigma Df(R_i(s)(u^-))r_i(R_i(s)(u^-))\,ds \qquad (1.45) \\ &= \lambda_i(u^-)\cdot[R_i(\sigma)(u^-) - u^-]. \end{aligned}$$

In this case, the Lax entropy conditions hold regardless of the sign of σ. Indeed,

$$\lambda_i(u^+) = \lambda_i(u^-, u^+) = \lambda_i(u^+). \qquad (1.46)$$

Observe that, according to (1.45), for linearly degenerate fields the shock and rarefaction curves actually coincide, i.e. $S_i(\sigma)(u_0) = R_i(\sigma)(u_0)$ for all σ.

The above results can be summarized as follows. For a fixed left state u^- and $i \in \{1, \ldots, n\}$ define the mixed curve

$$\Psi_i(\sigma)(u^-) = \begin{cases} R_i(\sigma)(u^-) & \text{if} \quad \sigma \geq 0, \\ S_i(\sigma)(u^-) & \text{if} \quad \sigma < 0. \end{cases} \qquad (1.47)$$

In the special case where $u^+ = \Psi_i(\sigma)(u^-)$ for some σ, the Riemann problem can then be solved by an elementary wave: a rarefaction, a shock or a contact discontinuity.

Relying on the previous analysis, the solution of the general Riemann problem (1.39) can now be obtained by finding intermediate states $\omega_0 = u^-$, $\omega_1, \ldots, \omega_n = u^+$ such that each pair of adiacent states ω_{i-1}, ω_i can be connected by an elementary wave, i. e.

$$\omega_i = \Psi_i(\sigma_i)(\omega_{i-1}) \qquad i = 1, \ldots, n. \qquad (1.48)$$

This can be done whenever u^+ is sufficiently close to u^-. Indeed, for $|u^+ - u^-|$ small, the implicit function theorem provides the existence of

unique wave strengths $\sigma_1, \dots \sigma_n$ such that (fig. 9)

$$u^+ = \Psi_n(\sigma_n) \circ \cdots \circ \Psi_1(\sigma_1)(u^-). \tag{1.49}$$

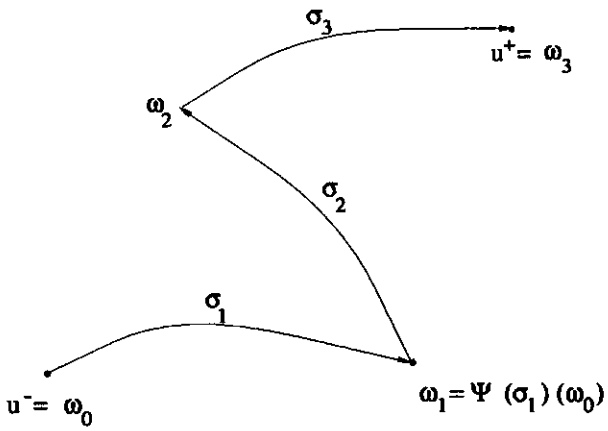

figure 9

In turn, these determine the intermediate states ω_i in (1.48). The solution to (1.39) is now obtained by piecing together the solutions of the n Riemann problems

$$u_t + f(u)_x = 0, \qquad u(0,x) = \begin{cases} \omega_{i-1} & \text{if} \quad x < 0, \\ \omega_i & \text{if} \quad x > 0 \end{cases} \tag{1.50}$$

on different sectors of the t-x plane. By construction, each problem has an entropy-admissible solution consisting of a simple wave of the i-th characteristic family. More precisely:

Case 1: The i-th characteristic field is genuinely nonlinear and $\sigma_i > 0$. Then the solution of (1.50) consists of a centered rarefaction wave. Its i-th characteristic speeds range over the interval $[\lambda_i^-,\ \lambda_i^+]$, defined as

$$\lambda_i^- \doteq \lambda_i(\omega_{i-1}), \qquad \lambda_i^+ \doteq \lambda_i(\omega_i). \tag{1.51}$$

Case 2: Either the i-th characteristic field is genuinely nonlinear and $\sigma_i \leq 0$, or else the i-th characteristic field is linearly degenerate (with σ_i arbitrary). Then the solution of (1.50) consists of an admissible shock or of a contact discontinuity, travelling with Rankine-Hugoniot speed

$$\lambda_i^- \doteq \lambda_i^+ \doteq \lambda_i(\omega_{i-1}, \omega_i). \tag{1.52}$$

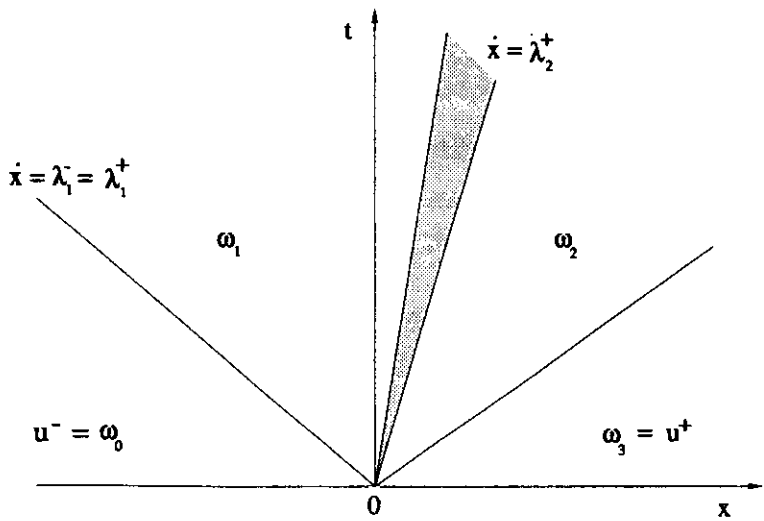

figure 10

The solution to the original problem (1.38) can now be constructed (fig. 10) by piecing together the solutions of the n Riemann problems (1.50), $i = 1, \ldots, n$. Indeed, for $\sigma_1, \ldots, \sigma_n$ sufficiently small, the speeds λ_i^-, λ_i^+ introduced at (1.51) or (1.52) remain close to the corresponding eigenvalues $\lambda_i(u^-)$ of the matrix $A(u^-)$. By strict hyperbolicity and continuity, we can thus assume that the n intervals $[\lambda_i^-, \lambda_i^+]$ are disjoint, i.e.

$$\lambda_1^- \leq \lambda_1^+ < \lambda_2^- \leq \lambda_2^+ < \cdots < \lambda_n^- \leq \lambda_n^+.$$

Therefore, a piecewise smooth solution $u : [0, \infty) \times \mathbb{R} \mapsto \mathbb{R}^n$ is well defined by the assignment:

$$u(t,x) = \begin{cases} u^- = \omega_0 & \text{if} \quad \frac{x}{t} \in]-\infty,\ \lambda_1^-[, \\ R_i(s)(\omega_{i-1}) & \text{if} \quad \frac{x}{t} = \lambda_i(R_i(s)(\omega_{i-1})) \in [\lambda_i^-,\ \lambda_i^+[, \\ \omega_i & \text{if} \quad \frac{x}{t} \in [\lambda_i^+,\ \lambda_{i+1}^-[, \\ u^+ = \omega_n & \text{if} \quad \frac{x}{t} \in [\lambda_n^+,\ \infty[\ . \end{cases} \tag{1.53}$$

Observe that this solution is self-similar, having the form $u(t,x) = \psi(x/t)$, with $\psi : \mathbb{R} \mapsto \mathbb{R}^n$ generally discontinuous.

Example 4. The 2×2 system of conservation laws

$$[u_1]_t + \left[\frac{u_1}{1+u_1+u_2}\right]_x = 0, \quad [u_2]_t + \left[\frac{u_2}{1+u_1+u_2}\right]_x = 0, \quad u_1, u_2 > 0, \tag{1.54}$$

is motivated by the study of two-component chromatography. Writing (1.54) in the quasilinear form (1.6), the eigenvalues and eigenvectors of $A(u)$ are found to be

$$\lambda_1(u) = \frac{1}{(1+u_1+u_2)^2}, \qquad \lambda_2(u) = \frac{1}{1+u_1+u_2},$$

$$r_1(u) = \frac{1}{\sqrt{u_1^2+u_2^2}} \cdot (-u_1, \ -u_2), \qquad r_2(u) = \frac{1}{\sqrt{2}} \cdot (1, \ -1).$$

The first characteristic field is genuinely nonlinear, the second is linearly degenerate. In this example, the two shock and rarefaction curves S_i, R_i always coincide, for $i = 1, 2$. Their computation is easy, because they are straight lines (fig. 11):

$$R_1(\sigma)(u) = u + \sigma r_1(u), \qquad R_2(\sigma)(u) = u + \sigma r_2(u). \tag{1.55}$$

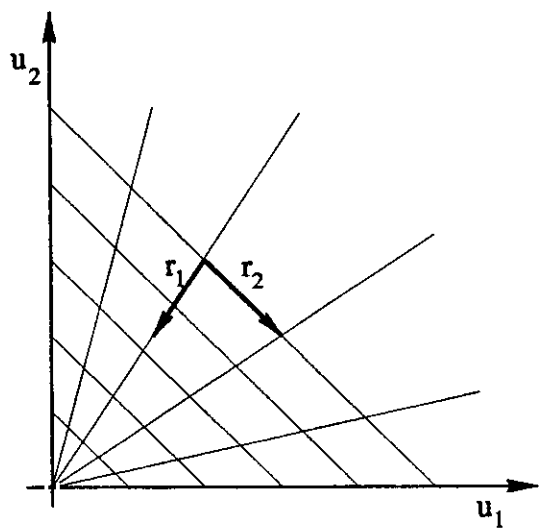

figure 11

Observe that the integral curves of the vector field r_1 are precisely the rays through the origin, while the integral curves of r_2 are the lines with slope -1. Now let two states $u^- = (u_1^-, u_2^-)$, $u^+ = (u_1^+, u_2^+)$ be given. To solve the Riemann problem (1.39), we first compute an intermediate state u^* such that $u^* = R_1(\sigma_1)(u^-)$, $u^+ = R_2(\sigma_2)(u^*)$ for some σ_1, σ_2. By (1.55), the components of u^* satisfy

$$u_1^* + u_2^* = u_1^+ + u_2^+, \qquad u_1^* u_2^- = u_1^- u_2^*.$$

The solution of the Riemann problem thus takes two different forms, depending on the sign of $\sigma_1 = \sqrt{(u_1^-)^2 + (u_2^-)^2} - \sqrt{(u_1^*)^2 + (u_2^*)^2}$.

Case 1: $\sigma_1 > 0$. Then the solution consists of a centered rarefaction wave of the first family and of a contact discontinuity of the second family:

$$u(t,x) = \begin{cases} u^- & \text{if} \quad x/t < \lambda_1(u^-), \\ su^* + (1-s)u^- & \text{if} \quad x/t = \lambda_1(su^* + (1-s)u^-),\ s \in [0,1], \\ u^* & \text{if} \quad \lambda_1(u^*) < x/t < \lambda_2(u^+), \\ u^+ & \text{if} \quad x/t \geq \lambda_2(u^+). \end{cases} \tag{1.56}$$

Case 2: $\sigma_1 \leq 0$. Then the solution contains a compressive shock of the first family (which vanishes if $\sigma_1 = 0$) and a contact discontinuity of the second family:

$$u(t,x) = \begin{cases} u^- & \text{if} \quad x/t < \lambda_1(u^-, u^*), \\ u^* & \text{if} \quad \lambda_1(u^-, u^*) \leq x/t < \lambda_2(u^+), \\ u^+ & \text{if} \quad x/t \geq \lambda_2(u^+). \end{cases} \tag{1.57}$$

Observe that $\lambda_2(u^*) = \lambda_2(u^+) = (1+u_1^+ + u_2^+)^{-1}$, because the second characteristic field is linearly degenerate. In this special case, since the integral curves of r_1 are straight lines, the shock speed in (1.57) can be computed as

$$\begin{aligned} \lambda_1(u^-, u^*) &= \int_0^1 \lambda_1(su^* + (1-s)u^-)\, ds \\ &= \int_0^1 [1 + s(u_1^* + u_2^*) + (1-s)(u_1^- + u_2^-)]^{-2}\, ds \\ &= \frac{1}{(1+u_1^*+u_2^*)(1+u_1^-+u_2^-)}\,. \end{aligned}$$

Example 5. A model for isentropic gas dynamics (in Lagrangian coordinates) is provided by the following 2×2 hyperbolic system:

$$v_t - u_x = 0, \qquad u_t + p(v)_x = 0. \tag{1.58}$$

Here $v > 0$ is the specific volume, i.e. $v = \rho^{-1}$ where ρ is the density, and u is the velocity. The function $p = p(v)$ gives the pressure in terms of the specific volume. It is thus natural to assume

$$p > 0, \qquad p' < 0, \qquad p'' > 0. \tag{1.59}$$

A typical choice, valid for most gases, is

$$p(v) = \frac{k}{v^\gamma}, \qquad 1 < \gamma < 3.$$

Here γ is called the *adiabatic gas constant.*

Introducing the vectors

$$U \doteq (v,\ u) \qquad F(U) \doteq (-u,\ p(v)),$$

the system (1.58) can be written in the standard form

$$U_t + [F(U)]_x = 0. \tag{1.60}$$

If the assumptions (1.59) hold, then the system (1.60) is strictly hyperbolic. Indeed, the Jacobian matrix

$$A(U) \doteq DF(U) = \begin{pmatrix} 0 & -1 \\ p'(v) & 0 \end{pmatrix}$$

has the two real distinct eigenvalues

$$\lambda_1 = -\sqrt{-p'(v)} < 0 < \sqrt{-p'(v)} = \lambda_2, \tag{1.61}$$

with corresponding (unnormalized) eigenvectors

$$r_1 = (1,\ \sqrt{-p'(v)}), \qquad r_2 = (-1,\ \sqrt{-p'(v)}). \tag{1.62}$$

We now study the Riemann problem for the system (1.60), with initial data

$$U(0,x) = \begin{cases} U^- = (v^-, u^-) & \text{if } x < 0, \\ U^+ = (v^+, u^+) & \text{if } x > 0, \end{cases} \tag{1.63}$$

assuming, that $v^-, v^+ > 0$.

By (1.62), the 1-rarefaction curve through U^- is obtained by solving the Cauchy problem

$$\frac{du}{dv} = \sqrt{-p'(v)}, \qquad u(v^-) = u^-.$$

This yields the curve

$$R_1 = \Big\{(v,u); \quad u - u^- = \int_{v^-}^{v} \sqrt{-p'(y)}\, dy\Big\}. \tag{1.64}$$

Similarly, the 2-rarefaction curve through the point U^- is

$$R_2 = \Big\{(v,u); \quad u - u^- = -\int_{v^-}^{v} \sqrt{-p'(y)}\, dy\Big\}. \tag{1.65}$$

Next, the shock curves S_1, S_2 through U^- are derived from the Rankine-Hugoniot conditions

$$\lambda(v - v^-) = -(u - u^-), \qquad \lambda(u - u^-) = p(v) - p(v^-). \tag{1.66}$$

Using the first equation in (1.66) to eliminate λ, these shock curves are computed as

$$S_1 = \Big\{(v,u); -(u-u^-)^2 = (v-v^-)\big(p(v)-p(v^-)\big), \lambda \doteq -\frac{u-u^-}{v-v^-} < 0\Big\} \tag{1.67}$$

$$S_2 = \Big\{(v,u); -(u-u^-)^2 = (v-v^-)\big(p(v)-p(v^-)\big), \lambda \doteq -\frac{u-u^-}{v-v^-} > 0\Big\} \tag{1.68}$$

Recalling (1.61)-(1.62) and the assumptions (1.59), we now compute the directional derivatives

$$(D\lambda_1)r_i = (D\lambda_2)r_2 = \frac{p''(v)}{2\sqrt{-p'(v)}} > 0. \tag{1.69}$$

From (1.69) it is clear that the Riemann problem (1.60), (1.63) admits a solution in the form of a centered rarefaction wave in the two cases $U^+ \in R_1$, $v^+ > v^-$, or else $U^+ \in R_2$, $v^+ < v^-$. On the other hand, a shock connecting U^- with U^+ will be admissible provided that either $U^+ \in S_1$ and $v^+ < v^-$, or else $U^+ \in S_2$ and $v^+ > v^-$.

Taking the above admissibility conditions into account, we thus obtain four lines originating from the point $U^- = (v^-, u^-)$, i.e. the two rarefaction curves

$$\sigma \mapsto R_1(\sigma),\ R_2(\sigma) \qquad \sigma \geq 0,$$

and the two shock curves

$$\sigma \mapsto S_1(\sigma),\ S_2(\sigma) \qquad \sigma \leq 0.$$

In turn, these curves divide a neighborhood of U^- into four regions (fig 12):

Ω_1,	bordering on	R_1, S_2,	Ω_2,	bordering on	R_1, R_2,
Ω_3,	bordering on	S_1, S_2,	Ω_4,	bordering on	S_1, R_2.

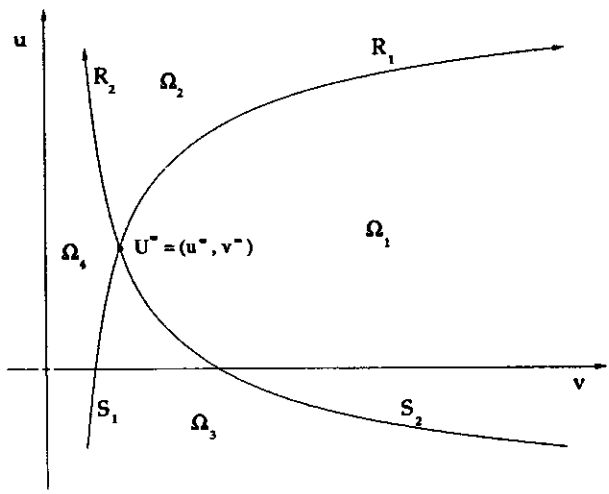

figure 12

For U^+ sufficiently close to U^-, the structure of the general solution to the Riemann problem is now determined by the location of the state U^+, with respect to the curves R_i, S_i (fig 13).

Case 1: $U^+ \in \Omega_1$. The solution consists of a 1-rarefaction wave and a 2-shock.

Case 2: $U^+ \in \Omega_2$. The solution consists of two centered rarefaction waves.

Case 3: $U^+ \in \Omega_3$. The solution consists of two shocks.

Case 4: $U^+ \in \Omega_4$. The solution consists of a 1-shock and a 2-rarefaction wave.

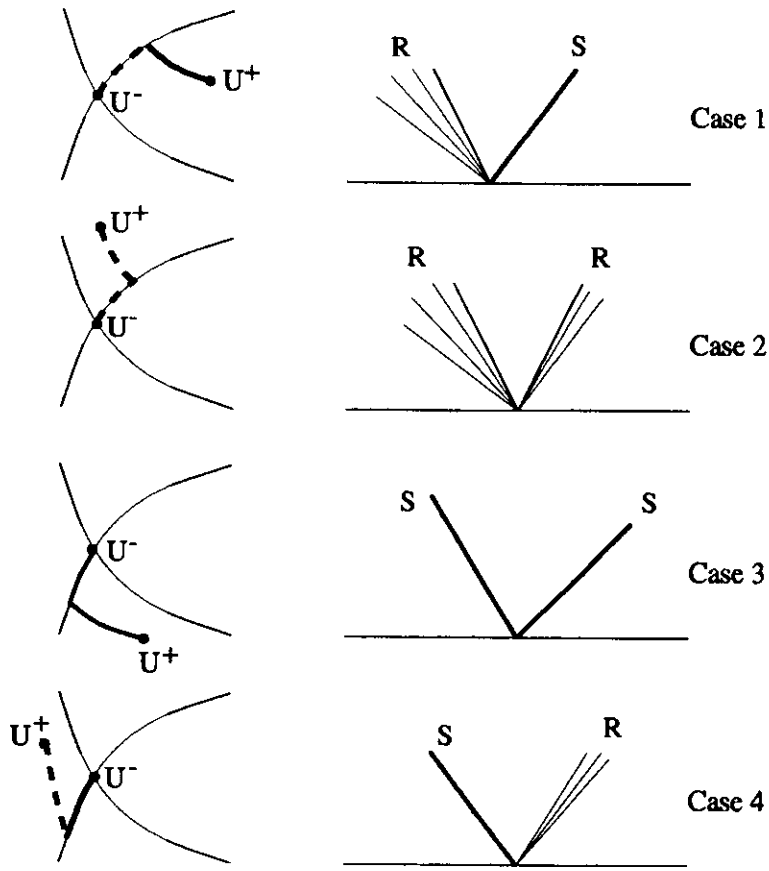

figure 13

2 Wave-front tracking approximations

The main goal of this chapter is to prove the global existence of a weak, entropy admissible solution to the Cauchy problem

$$u_t + f(u)_x = 0, \tag{2.1}$$

$$u(0,x) = \bar{u}(x), \tag{2.2}$$

for every integrable initial data $\bar{u}$ with sufficiently small total variation.

Theorem 1. *Let the system (2.1) be strictly hyperbolic and assume that each characteristic field is either linearly degenerate or genuinely nonlinear. Then there exists a constant $\delta > 0$ such that, for every initial condition $\bar{u} \in \mathbf{L}^1(\mathbb{R};\ \mathbb{R}^n)$ with*

$$Tot.Var.(\bar{u}) \leq \delta, \tag{2.3}$$

the Cauchy problem (2.1)-(2.2) has an entropy admissible weak solution $u = u(t,x)$ defined for all $t \geq 0$.

Theorem 1 was first proved in the fundamental paper of Glimm [15], constructing approximate solutions by means of a random restarting procedure.

Here we shall describe an alternative method for constructing approximate solutions, based on wave-front tracking. Roughly speaking, a front tracking ε-approximate solution (fig. 14) is a piecewise constant function $u = u(t,x)$ whose jumps are located along finitely many segments $x = x_\alpha(t)$ in the t-x plane. At each time $t > 0$, these jumps should approximately satisfy the Rankine-Hugoniot conditions

$$\sum_\alpha \Big|\dot{x}_\alpha[u(t,x_\alpha+) - u(t,x_\alpha-)] - [f(u(t,x_\alpha+)) - f(u(t,x_\alpha-))]\Big| = \mathcal{O}(\varepsilon).$$

If η is a convex entropy with flux q, recalling (1.27), at each time t one should also have

$$\sum_\alpha \Big\{[q(u(t,x_\alpha+)) - q(u(t,x_\alpha-))] - \dot{x}_\alpha[\eta(u(t,x_\alpha+)) - \eta(u(t,x_\alpha-))]\Big\} \leq \mathcal{O}(\varepsilon).$$

In practice, since we want to use these approximations for a detailed analysis of solutions, it is convenient to require a number of additional properties, described below.

Definition 1. *Given $\varepsilon > 0$, we say that $u : [0,\infty[\mapsto \mathbf{L}^1(\mathbb{R};\ \mathbb{R}^n)$ is an ε-approximate front tracking solution of (2.1) if the following holds:*

1. *As a function of two variables, $u = u(t,x)$ is piecewise constant, with discontinuities occurring along finitely many lines in the t-x plane. Only finitely many wave-front interactions occur, each involving exactly two incoming fronts. Jumps can be of three types: shocks (or contact*

discontinuities), rarefactions and non-physical waves, denoted as $\mathcal{J} = \mathcal{S} \cup \mathcal{R} \cup \mathcal{NP}$.

2. *Along each shock (or contact discontinuity)* $x = x_\alpha(t)$, $\alpha \in \mathcal{S}$, *the values* $u^- \doteq u(t, x_\alpha-)$ *and* $u^+ \doteq u(t, x_\alpha+)$ *are related by*

$$u^+ = S_{k_\alpha}(\sigma_\alpha)(u^-), \tag{2.4}$$

for some $k_\alpha \in \{1, \ldots, n\}$ *and some wave size* σ_α. *If the* k_α*-th family is genuinely nonlinear, then the entropy admissibility condition* $\sigma_\alpha < 0$ *also holds. Moreover, the speed of the shock front satisfies*

$$|\dot{x}_\alpha - \lambda_{k_\alpha}(u^+, u^-)| \leq \varepsilon. \tag{2.5}$$

3. *Along each rarefaction front* $x = x_\alpha(t)$, $\alpha \in \mathcal{R}$, *one has*

$$u^+ = R_{k_\alpha}(\sigma_\alpha)(u^-), \qquad \sigma_\alpha \in]0, \varepsilon] \tag{2.6}$$

for some genuinely nonlinear family k_α. *Moreover,*

$$|\dot{x}_\alpha(t) - \lambda_{k_\alpha}(u^+)| \leq \varepsilon. \tag{2.7}$$

4. *All non-physical fronts* $x = x_\alpha(t)$, $\alpha \in \mathcal{NP}$ *have the same speed:*

$$\dot{x}_\alpha(t) \equiv \hat{\lambda}, \tag{2.8}$$

where $\hat{\lambda}$ *is a fixed constant strictly greater than all characteristic speeds. The total strength of all non-physical fronts in* $u(t, \cdot)$ *remains uniformly small, namely*

$$\sum_{\alpha \in \mathcal{NP}} |u(t, x_\alpha+) - u(t, x_\alpha-)| \leq \varepsilon \qquad \text{for all } t \geq 0. \tag{2.9}$$

If, in addition, the initial value of u *satisfies*

$$\|u(0, \cdot) - \bar{u}\|_{\mathbf{L}^1} < \varepsilon, \tag{2.10}$$

we say that u *is an* ε*-approximate solution to the Cauchy problem (2.1)-(2.2).*

Toward a proof of Theorem 1, we shall first establish the existence of front tracking approximations.

Theorem 2. *For every $\varepsilon > 0$ and every initial data $\bar{u}$ with sufficiently small total variation, the Cauchy problem (2.1)-(2.2) admits an ε-approximate front tracking solution, defined for all $t \geq 0$.*

In a second step, we will show that a suitable sequence of front tracking approximations converges to a limit, providing an entropy weak solution to the Cauchy problem.

We now describe an algorithm which generates these front tracking approximations. The basic ideas were introduced in the papers of Dafermos [12] for scalar equations and Di Perna [13] for 2×2 systems, then extended in [1, 3, 21] to general $n \times n$ systems. The construction (fig. 14) starts at time $t = 0$ by taking a piecewise constant approximation $u(0, \cdot)$ of $\bar{u}$ satisfying (2.10), with Tot.Var.$\{u(0, \cdot)\} \leq$ Tot.Var.$\{\bar{u}\}$. Let $x_1 < \cdots < x_N$ be the points where $u(0, \cdot)$ is discontinuous. For each $\alpha = 1, \ldots, N$, the Riemann problem generated by the jump $(u(0, x_\alpha-),\ u(0, x_\alpha+))$ is approximately solved on a forward neighborhood of $(0, x_\alpha)$ in the t-x plane by a function of the form $u(t, x) = \varphi((x - x_\alpha)/t)$, with $\varphi : \mathbb{R} \mapsto \mathbb{R}^n$ piecewise constant. More precisely, if the exact solution of the Riemann problem contains only shocks and contact discontinuities, then we let u coincide with the exact solution, which is already piecewise constant. On the other hand, if centered rarefaction waves are present, they are approximated by a *centered rarefaction fan*, containing several small jumps travelling with a speed close to the characteristic speed.

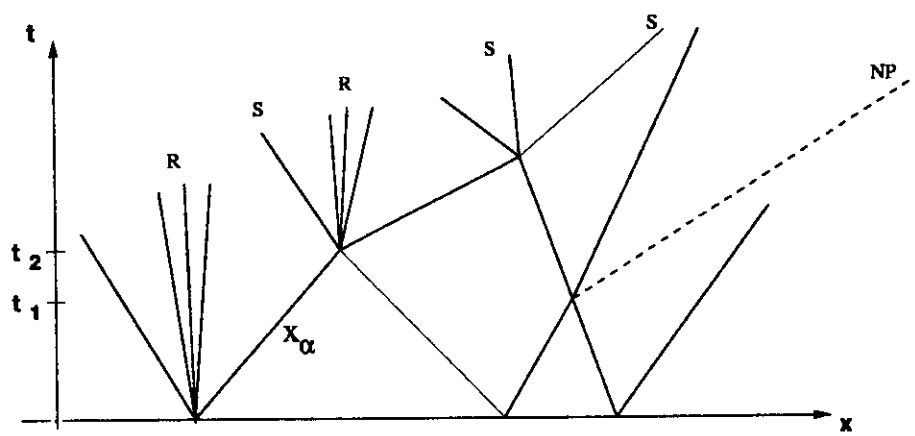

figure 14

The approximate solution u can then be prolonged until a time t_1 is reached, when the first set of interactions between two or more wave-fronts takes place. Since $u(t_1, \cdot)$ is still a piecewise constant function, the corresponding Riemann problems can again be approximately solved within the class of piecewise constant functions. The solution u is then continued up to a time t_2 where the second set of wave interactions takes place, etc...

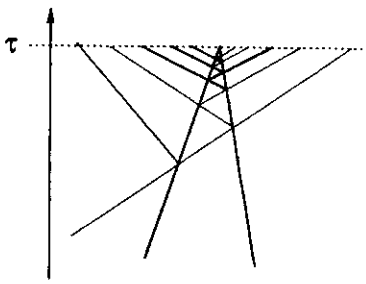

figure 15a

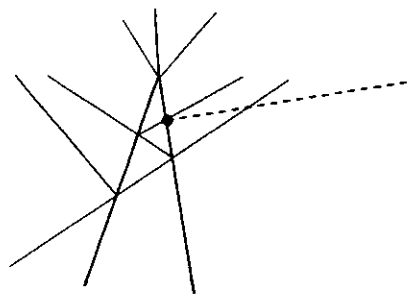

figure 15b

accurate Riemann solver

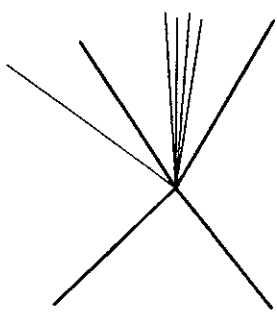

figure 16a

simplified Riemann solver

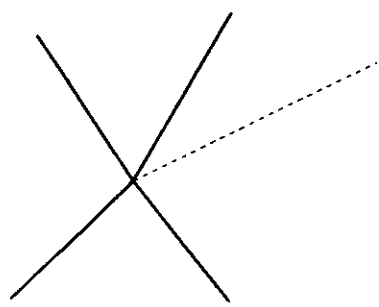

figure 16b

For general $n \times n$ systems, the main source of technical difficulty stems from the fact that the number of wave-fronts may approach infinity in finite time, in which case the construction would break down. To see this, observe that at a generic interaction point there will be two incoming fronts, while the number of outgoing fronts is n (if all waves generated by the Riemann problem are shocks or contact discontinuities), or even larger (if rarefaction waves are present). In turn, these

outgoing wave-fronts may quickly interact with several other fronts, generating more and more lines of discontinuity (see fig. 15a).

We thus need to modify the algorithm, to ensure that the number of fronts will not become infinite within finite time. Following [1, 3], we will use two different procedures for solving a Riemann problem within the class of piecewise constant functions: An Accurate Riemann Solver (fig. 16a), which introduces several new wave-fronts, and a Simplified Riemann Solver (fig. 16b), which involves a minimum number of outgoing fronts. In this second case, all new waves are lumped together in a single ***non-physical*** front, travelling with a fixed speed $\hat{\lambda}$ strictly larger than all characteristic speeds. The main feature of this algorithm is illustrated in fig. 15a-b. If all Riemann problems were solved accurately, the number of wave-fronts could approach infinity within a finite time τ (fig. 15a). However, since the total variation remains small, the new fronts generated by further interactions are very small. When their size becomes smaller than a threshold parameter $\rho > 0$, a Simplified Riemann Solver is used, which generates one single new (non-physical) front, with very small amplitude. The total number of fronts thus remains bounded for all times (fig. 15b).

Given a general Riemann problem at a point $(\bar{t}, \bar{x})$,

$$v_t + f(v)_x = 0, \qquad v(\bar{t}, x) = \begin{cases} u^- & \text{if } x < \bar{x}, \\ u^+ & \text{if } x > \bar{x}, \end{cases} \tag{2.11}$$

we now describe two procedures, which yield approximate solutions within the class of piecewise constant functions. As in the previous chapter, for a given state $u \in \mathbb{R}^n$, we denote respectively by

$$\sigma \mapsto R_i(\sigma)(u), \qquad \sigma \mapsto S_i(\sigma)(u) \qquad (i = 1, \dots, n) \tag{2.12}$$

the i-rarefaction and i-shock curve through the state u. Moreover, we set

$$\Psi_i(\sigma)(u) \doteq \begin{cases} R_i(\sigma)(u) & \text{if} \quad \sigma \geq 0, \\ S_i(\sigma)(u) & \text{if} \quad \sigma < 0. \end{cases} \tag{2.13}$$

Accurate Riemann Solver.

Given u^-, u^+, we first determine the states $\omega_0, \omega_1, \dots, \omega_n$ and parameter values $\sigma_1, \dots, \sigma_n$ such that

$$\omega_0 = u^-, \quad \omega_n = u^+, \, \omega_i = \Psi_i(\sigma_i)(\omega_{i-1}) \, i = 1, \dots, n. \tag{2.14}$$

Of course, $\omega_0, \ldots, \omega_n$ are the constant states present in the exact solution of the Riemann problem. If all jumps (ω_{i-1}, ω_i) were shocks or contact discontinuities, then the Riemann problem would have a piecewise constant solution with $\leq n$ lines of discontinuity. In the general case, the exact solution of (2.11) is not piecewise constant, because of the presence of rarefaction waves. These will be approximated by piecewise constant rarefaction fans, inserting additional states $\omega_{i,j}$ as follows.

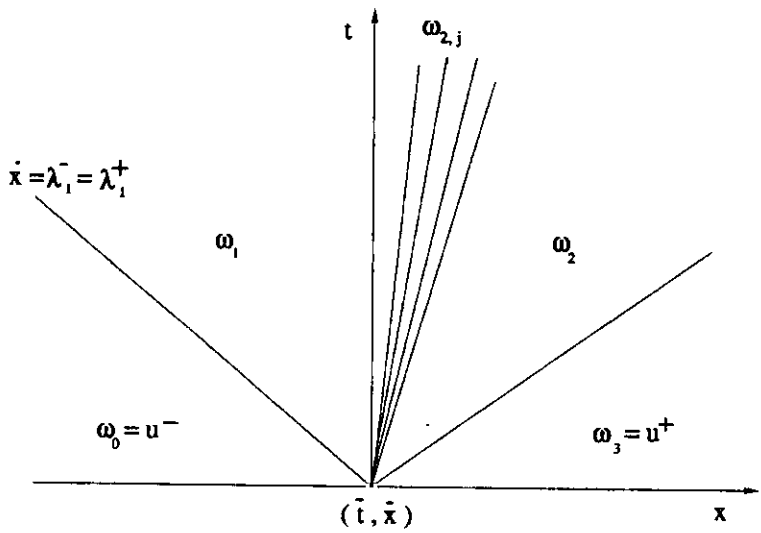

figure 17

Let $\delta > 0$ be a fixed small constant. If the i-th characteristic field is genuinely nonlinear and $\sigma_i > 0$, consider the integer

$$p_i \doteq 1 + [\![\sigma_i/\delta]\!], \tag{2.15}$$

where $[\![s]\!]$ denotes the integer part of s, i.e. the largest integer $\leq s$. For $j = 1, \ldots, p_i$, define

$$\omega_{i,j} = \Psi_i(j\sigma_i/p_i)(\omega_{i-1}), \qquad x_{i,j}(t) = \bar{x} + (t - \bar{t})\lambda_i(\omega_{i,j}). \tag{2.16}$$

On the other hand, if the i-th characteristic field is genuinely nonlinear and $\sigma_i \leq 0$, or if the i-th characteristic field is linearly degenerate (with σ_i arbitrary), define $p_i \doteq 1$ and

$$\omega_{i,1} = \omega_i, \qquad x_{i,1}(t) = \bar{x} + (t - \bar{t})\lambda_i(\omega_{i-1}, \omega_i). \tag{2.17}$$

Here $\lambda_i(\omega_{i-1}, \omega_i)$ is the Rankine-Hugoniot speed of a jump connecting ω_{i-1} with ω_i, so that

$$\lambda(\omega_{i-1}, \omega_i) \cdot (\omega_i - \omega_{i-1}) = f(\omega_i) - f(\omega_{i-1}). \tag{2.18}$$

As soon as the intermediate states $\omega_{i,j}$ and the locations $x_{i,j}(t)$ of the jumps have been determined by (2.16) and (2.17), we can define an approximate solution to the Riemann problem (2.11) by setting (fig. 17)

$$v(t,x) = \begin{cases} u^- & \text{if} \quad x < x_{1,1}(t), \\ u^+ & \text{if} \quad x > x_{n,p_n}(t), \\ \omega_i (= \omega_{i,p_i}) & \text{if} \quad x_{i,p_i}(t) < x < x_{i+1,1}(t), \\ \omega_{i,j} & \text{if} \quad x_{i,j}(t) < x < x_{i,j+1}(t) \; (j = 1, \dots, p_i - 1). \end{cases} \tag{2.19}$$

Observe that the difference between v and the exact self-similar solution of (2.11) is due to the fact that every centered i-rarefaction wave is here divided into equal parts and replaced by a rarefaction fan containing p_i wave-fronts. Because of (2.15), the strength of each one of these fronts is $< \delta$.

Simplified Riemann Solver.

Case 1: Let $j, j' \in \{1, \dots, n\}$ be the families of the two incoming wave-fronts, with $j \geq j'$. Assume that the left, middle and right states u_l, u_m, u_r before the interaction are related by

$$u_m = \Psi_j(\sigma)(u_l), \qquad u_r = \Psi_{j'}(\sigma')(u_m). \tag{2.20}$$

Define the auxiliary right state

$$\tilde{u}_r = \begin{cases} \Psi_j(\sigma) \circ \Psi_{j'}(\sigma')(u_l) & \text{if} \quad j > j', \\ \Psi_j(\sigma + \sigma')(u_r) & \text{if} \quad j = j'. \end{cases} \tag{2.21}$$

Let $\tilde{v} = \tilde{v}(t,x)$ be the piecewise constant solution of the Riemann problem with data $u_l, \tilde{u}_r$, constructed as in (1.19). Because of (2.21), the piecewise constant function $\tilde{v}$ contains exactly two wave-fronts of sizes σ', σ, if $j > j'$, or a single wave-front of size $\sigma + \sigma'$, if $j = j'$.

Of course, in general one has $\tilde{u}_r \neq u_r$. We let the jump $(\tilde{u}_r, u_r)$ travel with a fixed speed $\hat{\lambda}$, strictly bigger than all characteristic speeds. In a

forward neighborhood of the point $(\bar t, \bar x)$, we thus define an approximate solution v as follows (fig. 18a-b)

$$v(t,x) = \begin{cases} \tilde v(t,x) & \text{if} \quad x - \bar x < (t-\bar t)\hat\lambda, \\ \\ u_r & \text{if} \quad x - \bar x > (t-\bar t)\hat\lambda. \end{cases} \tag{2.22}$$

Observe that this simplified Riemann solver introduces a new *non-physical* wave-front, travelling with constant speed $\hat\lambda$. In turn, this front may interact with other (physical) fronts. One more case of interaction thus needs to be considered.

Case 2: A non-physical front hits from the left a wave-front of the i-characteristic family (fig. 18c), for some $i \in \{1, \ldots, n\}$.

Let u_l, u_m, u_r be the left, middle and right state before the interaction. If

$$u_r = \Psi_i(\sigma)(u_m), \tag{2.23}$$

define the auxiliary right state

$$\tilde u_r = \Psi_i(\sigma)(u_l). \tag{2.24}$$

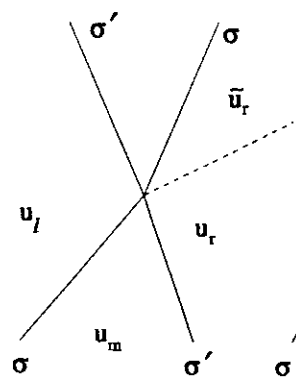

figure 18a

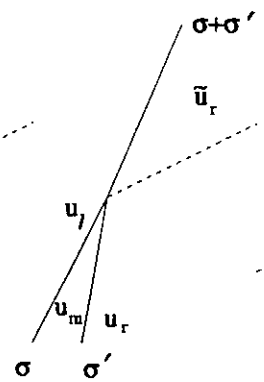

figure 18b

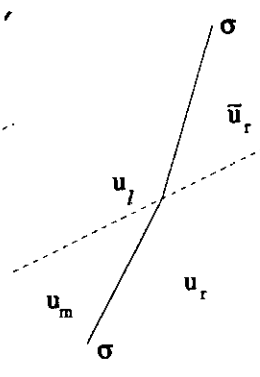

figure 18c

Call $\tilde v$ the solution to the Riemann problem with data $u_l, \tilde u_r$, constructed as in (2.19). Because of (2.24), $\tilde v$ will contain a single wave-front belonging to the i-th family, with size σ. Since $\tilde u_r \neq u_r$ in general, we let the jump $(\tilde u_r,\ u_r)$ travel with the fixed speed $\hat\lambda$. In a forward neighborhood of the point $(\bar t, \bar x)$, the approximate solution u is thus defined again according to (2.22).

By construction, all non-physical fronts travel with the same speed $\hat{\lambda}$, hence they never interact with each other. The above cases therefore cover all possible interactions between two wave-fronts.

To complete the description of the algorithm, it remains to specify which Riemann solver is used at any given interaction. The choice is made in connection with a threshold parameter $\rho > 0$:

- The accurate method is used at time $t = 0$, and at every interaction where the product of the strengths of the incoming waves is $|\sigma\sigma'| \geq \rho$.
- The simplified method is used at every interaction involving a non-physical wave-front, and also at interactions where the product of the strengths of the incoming waves is $|\sigma\sigma'| < \rho$.

In the above, we tacitly assumed that only two wave-fronts interact at any given point. This can always be achieved by an arbitrarily small change in the speed of one of the interacting fronts. We shall also adopt the provision that, in the Accurate Riemann Solver, rarefaction fronts of the same family of one of the incoming fronts are never partitioned (even if their strength is $> \delta$). This guarantees that every wave-front can be uniquely continued forward in time, unless it gets completely cancelled by interacting with another front of the same family and opposite sign.

The construction of an approximate solution thus involves three parameters:

- A fixed speed $\hat{\lambda}$, strictly larger than all characteristic speeds.
- A small constant $\delta > 0$, controlling the maximum strength of rarefaction fronts.
- A threshold parameter $\rho > 0$, determining whether the Accurate or the Simplified Riemann Solver is used.

This completes the definition of our algorithm. To prove Theorem 2, we now need to show that for any $\varepsilon > 0$, if the initial data $\bar{u}$ has small total variation, by a suitable choice of the parameters δ, ρ our algorithm will produce an ε-approximate solution defined for all $t \geq 0$. Observe that one can always solve the new Riemann problems generated

by wave-front interactions provided that the states u^-, u^+ are close to each other. A key part of the proof will thus consist in showing that the total variation of the approximate solution remains small for all times. An outline of the proof is given below.

1. Interaction Estimates. Whenever two wave-fronts interact, the new Riemann problem is solved in terms of a family of outgoing waves. Well known estimates [15, 24] state that the difference between the strengths of the corresponding incoming and outgoing fronts is of second order. More precisely, the following holds.

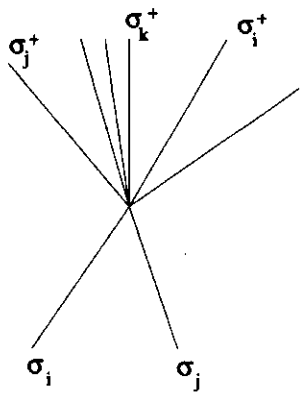

figure 19a

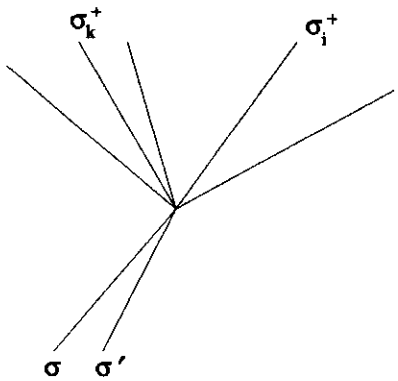

figure 19b

(i) Let σ_i, σ_j be the sizes of two incoming fronts, belonging to the distinct characteristic families $i > j$. Their interaction determines a Riemann problem (fig. 19a), whose solution consists of outgoing waves say of sizes $\sigma_1^+, \ldots, \sigma_n^+$. These are related to the incoming waves by the estimate

$$|\sigma_i^+ - \sigma_i| + |\sigma_j^+ - \sigma_j| + \sum_{k \neq i,j} |\sigma_k^+| = \mathcal{O}(1) \cdot |\sigma_i \sigma_j| \tag{2.25}$$

(ii) Let σ, σ' be the sizes of two incoming fronts, both belonging to the i-th characteristic family. As before, calling $\sigma_1^+, \ldots, \sigma_n^+$ the sizes of the outgoing waves generated by the corresponding Riemann problem (fig. 19b), one has

$$|\sigma_i^+ - \sigma - \sigma'| + \sum_{k \neq i} |\sigma_k^+| = \mathcal{O}(1) \cdot |\sigma\sigma'|(|\sigma| + |\sigma'|) \tag{2.26}$$

(iii) Let σ, σ' be the sizes of two incoming fronts, say of the families i, i'. Let u_l, u_m, u_r be the left, middle and right states before interaction, so that (2.20) holds. Introducing the auxiliary right state $\tilde{u}_r$ as in (2.21), one has (fig. 18a-b)

$$|\tilde{u}_r - u_r| = \mathcal{O}(1) \cdot |\sigma\sigma'|. \tag{2.27}$$

(iv) Let a non-physical front connecting the states u_l, u_m interact with an i-wave of size σ, connecting u_m, u_r, so that (1.13) holds. Defining the auxiliary right state $\tilde{u}_r$ as in (2.24), one has (fig. 18c)

$$|\tilde{u}_r - u_r| = \mathcal{O}(1) \cdot |\sigma||u_m - u_l|. \tag{2.28}$$

2. Bounds on the Total Variation. These a priori bounds are derived from the above estimates (2.25)–(2.28), using an interaction functional introduced in [15]. Let $u = u(t, x)$ be a piecewise constant approximate solution. At a fixed time t let x_α, $\alpha = 1, \ldots, N$, be the locations of the fronts in $u(t, \cdot)$. Moreover, let $|\sigma_\alpha|$ be the strength of the wave-front at x_α. In case of a non-physical front, one simply defines

$$|\sigma_\alpha| \doteq |u(t, x_\alpha+) - u(t, x_\alpha-)|. \tag{2.29}$$

In the following, for notational convenience we say that non-physical fronts belong to a $(n+1)$-th characteristic family.

As in [15], consider the two functionals

$$V(t) \doteq \sum_\alpha |\sigma_\alpha|, \tag{2.30}$$

measuring the *total strength of waves* in $u(t, \cdot)$, and

$$Q(t) \doteq \sum_{(\alpha,\beta)\in\mathcal{A}} |\sigma_\alpha \sigma_\beta| \tag{2.31}$$

measuring the *wave interaction potential*. In (2.31), the summation ranges over all couples of approaching wave-fronts. More precisely, we say that two fronts, located at points $x_\alpha < x_\beta$ and belonging to the characteristic families $k_\alpha, k_\beta \in \{1, \ldots, n+1\}$ respectively, are *approaching* if $k_\alpha > k_\beta$ or else if $k_\alpha = k_\beta$ and at least one of the waves is a genuinely nonlinear shock.

Now consider any approximate solution constructed by the front tracking algorithm. At every time τ where two fronts of strength $|\sigma|, |\sigma'|$ interact, the interaction estimates (2.25)–(2.28) yield

$$V(\tau+) - V(\tau-) = \mathcal{O}(1) \cdot |\sigma\sigma'|, \tag{2.32}$$

$$Q(\tau+) - Q(\tau-) = -|\sigma\sigma'| + \mathcal{O}(1) \cdot |\sigma\sigma'| \cdot V(\tau-). \tag{2.33}$$

Indeed, the two fronts σ, σ' are no longer approaching after time τ. If V remains sufficiently small, (2.33) implies

$$Q(\tau+) - Q(\tau-) \leq -\frac{|\sigma\sigma'|}{2}. \tag{2.34}$$

By (2.34) and (2.32) we can thus choose a constant C_0 large enough so that the quantity

$$\Upsilon(t) \doteq V(t) + C_0 Q(t)$$

decreases at every interaction time, provided that V remains sufficiently small. Observing that

$$V(t) = \mathcal{O}(1) \cdot \text{Tot.Var.}\{u(t,\cdot)\}, \qquad Q(t) \leq V^2(t), \tag{2.35}$$

we conclude that, if the total variation of the initial data $u(0,\cdot)$ is sufficiently small, then

$$V(t) + C_0 Q(t) \leq V(0) + C_0 Q(0) \qquad \text{for all } \ t \geq 0. \tag{2.36}$$

By (2.35), the total variation of $u(t,\cdot)$ thus remains small for all times $t \geq 0$. In particular, the approximate solutions of all Riemann problems generated by the interactions are well defined.

3. Bounds on the number of wave fronts. To prove that the total number of wave fronts remains finite, we recall that the Accurate Riemann Solver is used when the strengths of the interacting waves satisfy $|\sigma\sigma'| \geq \rho$. This can happen only finitely many times. Indeed, by (2.34) at such times one has

$$Q(\tau+) - Q(\tau-) \leq -\rho/2. \tag{2.37}$$

Therefore, new physical fronts are introduced only at a number $\leq 2Q(0)/\rho$ of interaction points, hence their total number is finite. In turn, a new

non-physical front is generated only when two physical fronts interact. Clearly, any two physical fronts can cross only once. Hence the total number of non-physical fronts is also finite.

The above steps **1–3** show that, for small enough initial data, the piecewise constant approximate solution is well defined for all times $t \geq 0$.

4. Strength of each rarefaction front is small. By construction, at a time t_0 where a new rarefaction front is introduced by the Accurate Riemann Solver, its size is $\sigma(t_0) \in]0, \delta]$. Observe that two rarefaction fronts of the same family never interact. If a rarefaction hits a shock of the same family, its size will decrease due to a cancellation. On the other hand, by subsequent interactions with fronts of other families, a rarefaction front may increase its initial strength. However, using the interaction estimates (2.25), it is not difficult to show that this strength remains uniformly bounded:

$$\sigma(t) = \mathcal{O}(1) \cdot \sigma(t_0) = \mathcal{O}(1) \cdot \delta \qquad \text{for all } t \geq t_0. \tag{2.38}$$

Choosing $\delta > 0$ sufficiently small, the right hand side of (2.38) remains smaller than ε.

5. Total strength of non-physical fronts is small. Toward this estimate, to each wave-front in u we attach an integer number, counting how many interactions were needed to produce such front. More precisely, the *generation order* of a front is inductively defined as follows (fig. 20).

- All fronts generated by the Riemann problems at the initial time $t = 0$ have generation order $k = 1$.

- Let two incoming fronts interact, say of the families $i, i' \in \{1, \ldots, n+1\}$, with generation orders k, k'. The orders of the outgoing fronts are then defined as follows.

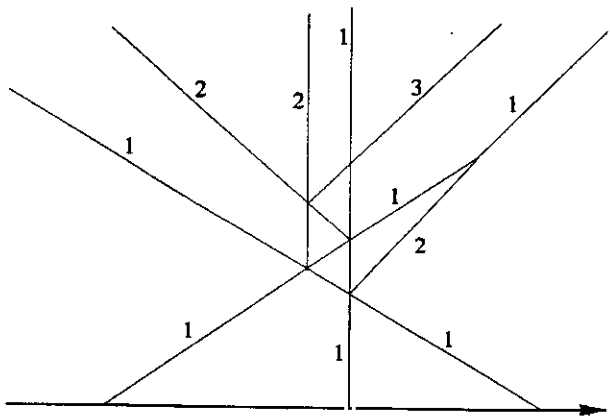

figure 20

Case 1: $i \neq i'$. Then

- the outgoing i-wave and i'-wave have the same orders k, k' as the incoming ones.
- the outgoing fronts of every other family $j \neq i, i'$ have order $\max\{k, k'\} + 1$.

Case 2: $i = i'$. Then

- the outgoing front of the i-th family has order $\min\{k, k'\}$,
- the outgoing fronts of every family $j \neq i$ have order $\max\{k, k'\} + 1$.

For $k \geq 1$, call $V_k(t)$ the sum at time t of the strengths of all waves of order $\geq k$. Moreover set $Q_k(t) = \sum |\sigma_\alpha \sigma_\beta|$, where the sum extends over all couples of approaching waves in $u(t, \cdot)$, say of order k_α, k_β, with $\max\{k_\alpha, k_\beta\} \geq k$. If the total variation is sufficiently small, from the interaction estimates (2.25)–(2.28) one obtains the a priori bounds

$$V_k(t) \leq C\gamma^k \qquad \text{for all } t > 0,\ k \geq 1, \tag{2.39}$$

for some constants C and $\gamma < 1$. Now let N be the number of wave-fronts in $u(0+, \cdot)$. At any time $t > 0$, the number of first order fronts in $u(t, \cdot)$ is thus $\leq N$. From each interaction between fronts of first order, recalling that rarefaction waves are partitioned into pieces of size

$< \delta$, a number $\mathcal{O}(1) \cdot 1/\delta$ of fronts of second order is generated. The total number of fronts of second order fronts is thus $\mathcal{O}(1) \cdot N^2/\delta$. By induction, the total number of of fronts of order $\leq k$ in $u(t, \cdot)$ can be estimated by some polynomial function of N, δ^{-1}, say

$$[\text{number of fronts of order } \leq k] \leq P_k(N, \delta^{-1}). \tag{2.40}$$

The particular form of P_k is of no interest here. By the interaction estimate (2.27), if at some time t_0 the Simplified Riemann Solver introduces a new non-physical front, the strength of this new front is

$$|\sigma(t_0)| = \mathcal{O}(1) \cdot |\sigma\sigma'| = \mathcal{O}(1) \cdot \rho. \tag{2.41}$$

By subsequent interactions, the strength of a non-physical front may increase. However, using the estimates (2.28), one can show that this strength remains uniformly bounded:

$$|\sigma(t)| = \mathcal{O}(1) \cdot |\sigma(t_0)| = \mathcal{O}(1) \cdot \rho \qquad \text{for all } t \geq t_0.$$

Therefore

$$[\text{maximum strength of each non-physical front in } u] \leq C'\rho \tag{2.42}$$

for some constant C'. To estimate the total strength of all non-physical waves in $u(t, \cdot)$ we keep track of the fronts having generation order $> k$ and $\leq k$ separately. Using (2.39), (2.40) and (2.42) we deduce

$$\begin{aligned}
&[\text{total strength of non-physical fronts in } u(t, \cdot)] \\
&\quad = \sum_{\text{order}(\alpha) > k} |\sigma_\alpha(t)| + \sum_{\text{order}(\alpha) \leq k} |\sigma_\alpha(t)| \\
&\quad \leq [\text{total strength of all fronts of order } > k] \\
&\qquad + [\text{maximum strength of non-physical fronts}] \\
&\qquad \cdot [\text{number of fronts of order } \leq k] \\
&\quad \leq C\gamma^k + C'\rho \cdot P_k(N, \delta^{-1}).
\end{aligned} \tag{2.43}$$

For any given $\varepsilon > 0$, since $\gamma < 1$ we can now choose k large enough so that $C\gamma^k < \varepsilon/2$. We then choose $\rho > 0$ small enough so that the second term on the right hand side of (2.43) is $< \varepsilon/2$. For all $t \geq 0$, this achieves

$$[\text{total strength of all non-physical fronts in } u(t, \cdot)] < \varepsilon, \tag{2.44}$$

completing the proof of Theorem 2.

We now work toward a proof of Theorem 1. Fix any sequence ε_ν decreasing to zero. For every $\nu \geq 1$, Theorem 2 yields the existence of an ε_ν-approximate solution u_ν of the Cauchy problem (2.1)-(2.2). By the previous analysis, these u_ν have uniformly bounded total variation. Moreover, the maps $t \mapsto u_\nu(t, \cdot)$ are uniformly Lipschitz continuous with values in $\mathbf{L}^1(\mathbb{R};\ \mathbb{R}^n)$. Indeed,

$$\begin{aligned} \|u_\nu(t) - u_\nu(s)\|_{\mathbf{L}^1} &\leq (t-s) \cdot [\text{total strength of all wave fronts}] \\ &\quad \cdot [\text{maximum speed}] \\ &\leq L \cdot (t-s) \end{aligned} \tag{2.45}$$

for some constant L independent of ν. We can thus apply Helly's compactness theorem and extract a subsequence which converges to some limit function u in $\mathbf{L}^1_{loc}$.

Since $\|u_\nu(0) - \bar{u}\|_{\mathbf{L}^1} \to 0$, by (2.45) the condition (2.2) clearly holds.

To prove that u is a weak solution of the Cauchy problem, it remains to show that, for every $\phi \in \mathcal{C}^1$ with compact support contained in the open half plane where $t > 0$, one has

$$\int_0^\infty \int_{-\infty}^\infty \phi_t(t,x)u(t,x) + \phi_x(t,x)f(u(t,x))\, dxdt = 0. \tag{2.46}$$

Since the u_ν are uniformly bounded and f is uniformly continuous on bounded sets, it suffices to prove that

$$\lim_{\nu \to 0} \left[\int_0^\infty \int_{-\infty}^\infty \left\{ \phi_t(t,x)u_\nu(t,x) + \phi_x(t,x)f(u_\nu(t,x)) \right\} dxdt \right] = 0. \tag{2.47}$$

Choose $T > 0$ such that $\phi(t,x) = 0$ whenever $t \notin]0,T[$. For a fixed ν, at any time t call $x_1(t) < \cdots < x_N(t)$ the points where $u_\nu(t, \cdot)$ has a jump, and set

$$\Delta u_\nu(t, x_\alpha) \doteq u_\nu(t, x_\alpha+) - u_\nu(t, x_\alpha-),$$

$$\Delta f(u_\nu(t, x_\alpha)) \doteq f(u_\nu(t, x_\alpha+)) - f(u_\nu(t, x_\alpha-)).$$

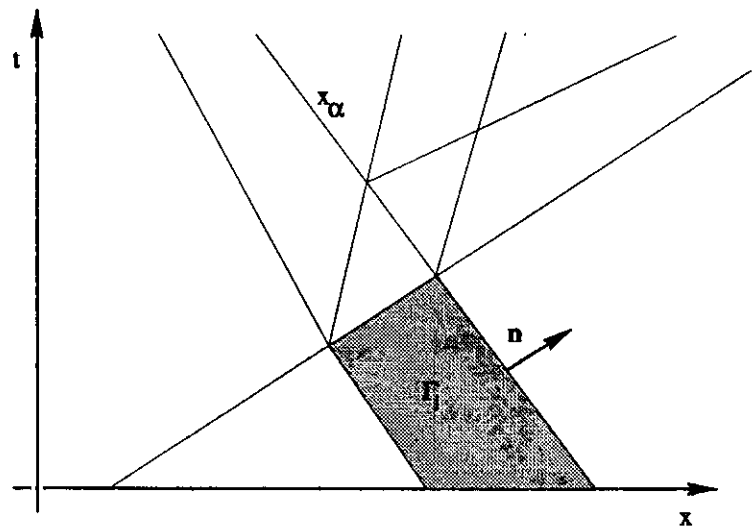

figure 21

Observe that the polygonal lines $x = x_\alpha(t)$ subdivide the strip $[0,T] \times \mathbb{R}$ into finitely many regions Γ_j where u_ν is constant. Introducing the vector

$$\Phi \doteq (\phi \cdot u_\nu,\ \phi \cdot f(u_\nu)),$$

by the divergence theorem the double integral in (2.47) can be written as

$$\sum_j \iint_{\Gamma_j} \operatorname{div} \Phi(t,x)\, dxdt = \sum_j \int_{\partial\Gamma_j} \Phi \cdot \mathbf{n}\, d\sigma. \tag{2.48}$$

Here $\partial\Gamma_j$ is the oriented boundary of Γ_j, while $\mathbf{n}$ denotes an outer normal (fig. 21). Observe that $\mathbf{n}d\sigma = \pm(\dot{x}_\alpha, -1)dt$ along each polygonal line $x = x_\alpha(t)$, while $\phi(t,x) = 0$ along the lines $t = 0, t = T$. By (2.48) the expression within square brackets in (2.47) is computed by

$$\int_0^T \sum_\alpha \Big[\dot{x}_\alpha(t) \cdot \Delta u_\nu(t, x_\alpha) - \Delta f(u_\nu(t, x_\alpha))\Big] \phi(t, x_\alpha(t))\, dt. \tag{2.49}$$

To estimate the above integral, let $|\sigma_\alpha|$ be the strength of the wave at x_α. If this wave is a shock, a rarefaction or contact discontinuity, by (2.4)–(2.7) one has

$$\Big|\dot{x}_\alpha(t) \cdot \Delta u_\nu(t, x_\alpha) - \Delta f(u_\nu(t, x_\alpha))\Big| = \mathcal{O}(1) \cdot \varepsilon_\nu |\sigma_\alpha|. \tag{2.50}$$

On the other hand, if the wave at x_α is non-physical with strength $|\sigma_\alpha|$, then

$$\Big|\dot{x}_\alpha \cdot \Delta u_\nu(t, x_\alpha) - \Delta f(u_\nu(t, x_\alpha))\Big| = \mathcal{O}(1) \cdot |\sigma_\alpha|. \tag{2.51}$$

We now split the summation in (2.49), considering physical (shocks, contacts or rarefactions) and nonphysical waves separately:

$$\begin{aligned} \limsup_{\nu\to\infty} \Big| \sum_{\alpha\in\mathcal{S}\cup\mathcal{R}\cup\mathcal{NP}} \Big[\dot{x}_\alpha(t)\cdot\Delta u_\nu(t,x_\alpha) \\ -\Delta f(u_\nu(t,x_\alpha))\Big]\phi(t,x_\alpha(t))\Big| \\ \leq \Big(\max_{t,x}|\phi(t,x)|\Big)\cdot \limsup_{\nu\to\infty}\Big\{\mathcal{O}(1)\cdot\sum_{\alpha\in\mathcal{S}\cup\mathcal{R}}\varepsilon_\nu|\sigma_\alpha| \\ +\mathcal{O}(1)\cdot\sum_{\alpha\in\mathcal{NP}}|\sigma_\alpha|\Big\} = 0. \end{aligned} \tag{2.52}$$

Indeed, the total strength of waves in u_ν remains uniformly bounded, while the amount of non-physical waves by (2.44) approaches zero as $\varepsilon_\nu \to 0$. The limit (2.47) now follows from (2.52). Therefore, u is a weak solution to the Cauchy problem. In the presence of a convex entropy η with entropy flux q, an entirely similar argument shows that the inequality (1.26) is also satisfied.

3 A semigroup of solutions

The analysis in the previous chapter has shown the existence of a global entropy weak solution of the Cauchy problem for every initial data with sufficiently small total variation. More precisely, recalling the definitions (2.30)-(2.31), consider a domain of the form

$$\begin{aligned} \mathcal{D} = cl\Big\{u\in \mathbf{L}^1(\mathbb{R};\mathbb{R}^n);\quad u \text{ is piecewise constant,} \\ \Upsilon(u)\doteq V(u)+C_0\cdot Q(u)<\delta_0\Big\}, \end{aligned} \tag{3.1}$$

where cl denotes closure in $\mathbf{L}^1$. With a suitable choice of the constants C_0 and $\delta_0 > 0$, the proofs of Theorems 1, 2 show that, for every $\bar{u} \in \mathcal{D}$, one can construct a sequence of ε-approximate front tracking solutions converging to a weak solution u taking values inside $\mathcal{D}$. Observe that, since the proof of convergence relied on a compactness argument, no

information was obtained on the uniqueness of the limit. The main goal of the present chapter is to show that this limit is unique and depends continuously on the initial data:

Theorem 3. *For every $\bar{u} \in \mathcal{D}$, as $\varepsilon \to 0$ every sequence of ε-approximate solutions $u_\varepsilon : [0, \infty[\mapsto \mathcal{D}$ of the Cauchy problem (2.1)-(2.2) converges to a unique limit solution $u : [0, \infty[\mapsto \mathcal{D}$. The map $(\bar{u}, t) \mapsto u(t, \cdot) \doteq S_t \bar{u}$ is a uniformly Lipschitz semigroup, i.e.:*

$$S_0 \bar{u} = \bar{u}, \qquad S_s(S_t \bar{u}) = S_{s+t} \bar{u}, \tag{3.2}$$

$$\|S_t \bar{u} - S_s \bar{v}\|_{\mathbf{L}^1} \leq L \cdot (\|\bar{u} - \bar{v}\|_{\mathbf{L}^1} + |t - s|) \text{ for all } \bar{u}, \bar{v} \in \mathcal{D}, \ s, t \geq 0. \tag{3.3}$$

A construction of the semigroup was first carried out in [2] for linearly degenerate systems, then in [6] for 2×2 systems and in [7] for general $n \times n$ systems. All these earlier estimates were based on a linearization method. In order to estimate how the distance between two solutions u, v varies in time, one constructs a one-parameter family of solutions u^θ joining u with v, as shown in fig. 22. At any time $t \in [0, T]$, the distance $\|u(t) - v(t)\|_{\mathbf{L}^1}$ is thus bounded by the length of the curve $\gamma_t : \theta \mapsto u^\theta(t)$. In turn, as long as all solutions u^θ remain sufficiently regular, the length of γ_t can be computed by integrating the norm of a generalized tangent vector $\mathbf{v}$. The advantage of this approach is that tangent vectors satisfy a linearized evolution equation. From a uniform a-priori estimate on the norm of these tangent vectors, one obtains a bound on the length of γ_T and hence on the distance between $u(T)$ and $v(T)$. Unfortunately, this approach is hampered by the possible loss of regularity of the solutions u^θ. In order to retain the minimal regularity (piecewise Lipschitz continuity) required for the existence of tangent vectors, in [6, 7] various approximation and restarting procedures had to be devised. These yield entirely rigorous proofs, but at the price of heavy technicalities.

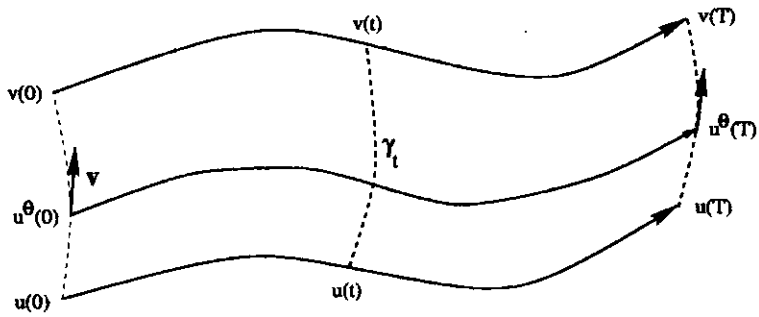

figure 22

In the remainder of this chapter, we will thus follow the new approach of Liu and Yang [19, 20] in its simplified version [11].

To prove the uniqueness of the limit of front tracking approximations, we need to estimate the distance between any two ε-approximate solutions u, v of (2.1). For this purpose, following [11] we introduce a functional $\Phi = \Phi(u, v)$, uniformly equivalent to the $\mathbf{L}^1$ distance, which is "almost decreasing" along pairs of solutions. Recalling the construction of shock curves at (1.33), given u, v, consider the scalar functions q_i defined implicitly by

$$v(x) = S_n(q_n(x)) \circ \cdots \circ S_1(q_1(x))(u(x)). \tag{3.4}$$

Intuitively, $q_i(x)$ can be regarded as the strength of the i-shock wave in the jump $(u(x),\ v(x))$. On a compact neighborhood of the origin, we clearly have

$$\frac{1}{C_1} \cdot |v(x) - u(x)| \leq \sum_{i=1}^{n} |q_i(x)| \leq C_1 \cdot |v(x) - u(x)| \tag{3.5}$$

for some constant C_1. We now consider the functional

$$\Phi(u, v) \doteq \sum_{i=1}^{n} \int_{-\infty}^{\infty} |q_i(x)| W_i(x)\, dx, \tag{3.6}$$

where the weights W_i are defined by setting:

$$\begin{aligned} W_i(x) \ &\doteq\ 1 + \kappa_1 \cdot [\text{ total strength of waves in } u \text{ and in } v \\ &\qquad \text{which approach the } i\text{-wave } q_i(x)] \\ &\qquad + \kappa_2 \cdot [\text{ wave interaction potentials of } u \text{ and of } v] \\ &\doteq\ 1 + \kappa_1 A_i(x) + \kappa_2 [Q(u) + Q(v)]. \end{aligned} \tag{3.7}$$

The amount of waves approaching $q_i(x)$ is defined as follows. If the i-shock and i-rarefaction curves coincide, we simply take

$$A_i(x) \doteq \left[\sum_{x_\alpha < x,\ i < k_\alpha \leq n} + \sum_{x_\alpha > x,\ 1 \leq k_\alpha < i} \right] |\sigma_\alpha|. \tag{3.8}$$

The summations here extend to waves both of u and of v. According to [25], the definition (3.8) applies if the i-th field is linearly degenerate, or else if all i-rarefaction curves are straight lines. On the other hand, if the i-th field is genuinely nonlinear with shock and rarefactions curves not coinciding, our definition of A_i will contain an additional term, accounting for waves in u and in v of the same i-th family:

$$\begin{aligned} A_i(x) \doteq & \left[\sum_{\substack{\alpha \in \mathcal{J}(u) \cup \mathcal{J}(v) \\ x_\alpha < x,\ i < k_\alpha \leq n}} + \sum_{\substack{\alpha \in \mathcal{J}(u) \cup \mathcal{J}(v) \\ x_\alpha > x,\ 1 \leq k_\alpha < i}} \right] |\sigma_\alpha| \\ + & \begin{cases} \left[\sum_{\substack{k_\alpha = i \\ \alpha \in \mathcal{J}(u),\ x_\alpha < x}} + \sum_{\substack{k_\alpha = i \\ \alpha \in \mathcal{J}(v),\ x_\alpha > x}} \right] |\sigma_\alpha| & \text{if } q_i(x) < 0, \\ \left[\sum_{\substack{k_\alpha = i \\ \alpha \in \mathcal{J}(v),\ x_\alpha < x}} + \sum_{\substack{k_\alpha = i \\ \alpha \in \mathcal{J}(u),\ x_\alpha > x}} \right] |\sigma_\alpha| & \text{if } q_i(x) > 0. \end{cases} \end{aligned} \tag{3.9}$$

Here and in the sequel, $\mathcal{J}(u)$ and $\mathcal{J}(v)$ denote the sets of all jumps in u and in v, while $\mathcal{J} \doteq \mathcal{J}(u) \cup \mathcal{J}(v)$. We recall that $k_\alpha \in \{1, \ldots, n+1\}$ is the family of the jump located at x_α with size σ_α. Notice that the strengths of non-physical waves do enter in the definition of Q. Indeed, a non-physical front located at x_α approaches all shock and rarefaction fronts located at points $x_\beta > x_\alpha$. On the other hand, non-physical fronts play no role in the definition of A_i.

The values of the large constants κ_1, κ_2 in (3.7) will be specified later. Observe that, as soon as these constants have been assigned, we can then impose a suitably small bound on the total variation of u, v so that

$$1 \leq W_i(x) \leq 2 \qquad \text{for all } i, x. \tag{3.10}$$

From (3.5), (3.6) and (3.10) it thus follows

$$\frac{1}{C_1}\cdot\|v-u\|_{\mathbf{L}^1}\leq\Phi(u,v)\leq 2C_1\cdot\|v-u\|_{\mathbf{L}^1}\,. \tag{3.11}$$

Recalling the definition $\Upsilon(u)\doteq V(u)+C_0Q(u)$, the basic $\mathbf{L}^1$ stability estimate for front tracking approximations can now be stated as follows.

Theorem 4. *For suitable constants $C_2,\kappa_1,\kappa_2,\delta_0>0$ the following holds. Let u,v be ε-approximate front tracking solutions of (1.1) constructed by the algorithm in Chapter 2, with*

$$\Upsilon(u(t))<\delta_0,\qquad \Upsilon(v(t))<\delta_0\qquad \text{for all } t\geq 0. \tag{3.12}$$

Then the functional Φ in (3.6)-(3.9) satisfies

$$\Phi(u(t),\,v(t))-\Phi(u(s),\,v(s))\leq C_2\varepsilon(t-s)\ \text{for all}\quad 0\leq s<t. \tag{3.13}$$

Relying on the above estimate, a proof of Theorem 3 can be easily worked out. Indeed, let $\bar u\in\mathcal{D}$ be given. Consider any sequence $\{u_\nu\}_{\nu\geq 1}$, such that each u_ν is a front tracking ε_ν-approximate solution of Cauchy problem (2.1)-(2.2), with

$$\lim_{\nu\to\infty}\varepsilon_\nu=0,\qquad \Upsilon(u_\nu(t))<\delta_0\qquad \text{for all } t\geq 0,\ \nu\geq 1.$$

For every $\mu,\nu\geq 1$ and $t\geq 0$, by (3.11) and (3.13) it now follows

$$\begin{aligned}\|u_\mu(t)-u_\nu(t)\|_{\mathbf{L}^1}&\leq C_1\cdot\Phi(u_\mu(t),\,u_\nu(t))\\&\leq C_1\cdot\Big[\Phi(u_\mu(0),\,u_\nu(0))+C_2t\cdot\max\{\varepsilon_\mu,\,\varepsilon_\nu\}\Big]\\&\leq 2C_1^2\|u_\mu(0)-u_\nu(0)\|_{\mathbf{L}^1}+C_1C_2t\cdot\max\{\varepsilon_\mu,\,\varepsilon_\nu\}.\end{aligned} \tag{3.14}$$

Since the right hand side of (3.14) approaches zero as $\mu,\nu\to\infty$, the sequence is Cauchy and converges to a unique limit. The semigroup property (3.2) is an immediate consequence of uniqueness. Finally, let $\bar u,\bar v\in\mathcal{D}$ be given. For each $\nu\geq 1$, let u_ν,v_ν be front tracking ε_ν-approximate solutions of (2.1) with

$$\|u_\nu(0)-\bar u\|_{\mathbf{L}^1}<\varepsilon_\nu,\ \|v_\nu(0)-\bar v\|_{\mathbf{L}^1}<\varepsilon_\nu,\ \lim_{\nu\to\infty}\varepsilon_\nu=0. \tag{3.15}$$

Using again (3.11) and (3.13) we deduce

$$\begin{aligned} \|u_\nu(t) - v_\nu(t)\|_{\mathbf{L}^1} &\leq C_1 \cdot \Phi(u_\nu(t),\, v_\nu(t)) \\ &\leq C_1 \cdot \Big[\Phi(u_\nu(0),\, v_\nu(0)) + C_2 t\varepsilon_\nu\Big] \\ &\leq 2C_1^2 \|u_\nu(0) - v_\nu(0)\|_{\mathbf{L}^1} + C_1 C_2 t\varepsilon_\nu. \end{aligned} \tag{3.16}$$

Letting $\nu \to \infty$, by (3.15) it follows

$$\|u(t) - v(t)\|_{\mathbf{L}^1} \leq 2C_1^2 \cdot \|\bar{u} - \bar{v}\|_{\mathbf{L}^1}\,. \tag{3.17}$$

This establishes the uniform Lipschitz continuity of the semigroup with respect to the initial data. Recalling (2.45), the Lipschitz continuity with respect to time is clear. This completes the proof of Theorem 3.

In the remainder of this chapter we will sketch the main ideas in the proof of Theorem 4. The key point is to understand how the functional Φ evolves in time. In connection with (3.4), at each x define the intermediate states $\omega_0(x) = u(x), \omega_1(x), \ldots, \omega_n(x) = v(x)$ by setting

$$\omega_i(x) \doteq S_i(q_i(x)) \circ\, S_{i-1}(q_{i-1}(x)) \circ\, \cdots \circ S_1(q_1(x))(u(x)). \tag{3.18}$$

Moreover, call

$$\lambda_i(x) \doteq \lambda_i(\omega_{i-1}(x),\, \omega_i(x)) \tag{3.19}$$

the speed of the i-shock connecting $\omega_{i-1}(x)$ with $\omega_i(x)$. A direct computation now yields

$$\begin{aligned} \tfrac{d}{dt}\Phi(u(t),\, v(t)) &= \textstyle\sum_{\alpha\in\mathcal{J}} \sum_{i=1}^n \Big\{ |q_i(x_\alpha-)| W_i(x_\alpha-) \\ &\qquad -|q_i(x_\alpha+)| W_i(x_\alpha+) \Big\} \cdot \dot{x}_\alpha \\ &= \textstyle\sum_{\alpha\in\mathcal{J}} \sum_{i=1}^n \Big\{ |q_i^{\alpha+}| W_i^{\alpha+} (\lambda_i^{\alpha+} - \dot{x}_\alpha) \\ &\qquad -|q_i^{\alpha-}| W_i^{\alpha-} (\lambda_i^{\alpha-} - \dot{x}_\alpha) \Big\}, \end{aligned} \tag{3.20}$$

with obvious meaning of notations. We regard the quantity $|q_i(x)|\lambda_i(x)$ as the flux of the i-th component of $|v - u|$ at x. For $x_{\alpha-1} < x < x_\alpha$, one clearly has

$$|q_i^{(\alpha-1)+}|\, \lambda_i^{(\alpha-1)+} W_i^{(\alpha-1)+} = |q_i(x)|\lambda_i(x) W_i(x) = |q_i^{\alpha-}|\, \lambda_i^{\alpha-} W_i^{\alpha-}.$$

Moreover, the assumption $u(t), v(t) \in \mathbf{L}^1$ and piecewise constant implies $q_i(t,x) \equiv 0$ for x outside a bounded interval. This allowed us to add and subtract the above terms in (3.20), without changing the overall sum.

In connection with (3.20), for each jump point $\alpha \in \mathcal{J}$ and every $i = 1, \ldots, n$, define

$$E_{\alpha,i} \doteq |q_i^{\alpha+}| W_i^{\alpha+}(\lambda_i^{\alpha+} - \dot{x}_\alpha) - |q_i^{\alpha-}| W_i^{\alpha-}(\lambda_i^{\alpha-} - \dot{x}_\alpha). \tag{3.21}$$

Our main goal will be to establish the bounds

$$\sum_{i=1}^{n} E_{\alpha,i} \leq \mathcal{O}(1) \cdot |\sigma_\alpha| \qquad \alpha \in \mathcal{NP}, \tag{3.22}$$

$$\sum_{i=1}^{n} E_{\alpha,i} \leq \mathcal{O}(1) \cdot \varepsilon |\sigma_\alpha| \qquad \alpha \in \mathcal{R} \cup \mathcal{S}. \tag{3.23}$$

As usual, by the Landau symbol $\mathcal{O}(1)$ we denote a quantity whose absolute value satisfies a uniform bound, depending only on the system (2.1). In particular, this bound does not depend on ε or on the functions u, v. It is also independent of the choice of the constants κ_1, κ_2 in (3.7).

From (3.22)-(3.23), recalling (2.9) and the uniform bounds (3.12) on the total strength of waves, one obtains the key estimate

$$\frac{d}{dt}\Phi(u(t),\ v(t)) \leq \mathcal{O}(1) \cdot \varepsilon. \tag{3.24}$$

If the constant κ_2 in (3.7) is chosen large enough, by the interaction estimates (2.25)–(2.28) all weight functions $W_i(x)$ will decrease at each time τ where two fronts of u or two fronts of v interact. Integrating (3.24) over the interval $[s, t]$ we therefore obtain

$$\Phi(u(t),\ v(t)) \leq \Phi(u(s),\ v(s)) + \mathcal{O}(1) \cdot \varepsilon(t - s), \tag{3.25}$$

proving the theorem. All the remaining work is thus aimed at establishing (3.22)-(3.23).

If $\alpha \in \mathcal{NP}$, calling σ_α the strength of this jump as in (2.29), for $i = 1, \ldots, n$ one has the easy estimates

$$\begin{array}{lll} q_i^{\alpha+} - q_i^{\alpha-} & = \mathcal{O}(1) \cdot \sigma_\alpha, & \\ \lambda_i^{\alpha+} - \lambda_i^{\alpha-} & = \mathcal{O}(1) \cdot \sigma_\alpha. & \\ W_i^{\alpha+} - W_i^{\alpha-} & = 0 & \text{if } \ q_i^{\alpha+} \cdot q_i^{\alpha-} > 0 \end{array} \tag{3.26}$$

Therefore, writing

$$\begin{aligned} E_{\alpha,i} = &(|q_i^{\alpha+}| - |q_i^{\alpha-}|)W_i^{\alpha+}(\lambda_i^{\alpha+} - \dot{x}_\alpha) \\ &+|q_i^{\alpha-}|(W_i^{\alpha+} - W_i^{\alpha-})(\lambda_i^{\alpha+} - \dot{x}_\alpha) \\ &+|q_i^{\alpha-}|W_i^{\alpha-}(\lambda_i^{\alpha+} - \lambda_i^{\alpha-}), \end{aligned} \tag{3.27}$$

the estimate (3.22) is clear.

The proof of (3.23) requires more work. Instead of writing down all computations, we will try to convey the main ideas with the help of a few pictures. For all details we refer to [11]. Given two piecewise constant functions u, v with compact support, for $i = 1, \dots, n$ we can define the scalar components u_i, v_i as in [19], by induction on the jump points of u, v. We start by setting $u_i(-\infty) = v_i(-\infty) = 0$. If $x_\alpha \in \mathcal{J}(u)$ is a jump point of u, then we let v_i be constant across x_α and set

$$u_i(x_\alpha+) \doteq u_i(x_\alpha-) - [q_i(x_\alpha+) - q_i(x_\alpha-)].$$

On the other hand, if $x_\alpha \in \mathcal{J}(v)$ is a jump point of v, then we let u_i be constant across x_α and set

$$v_i(x_\alpha+) \doteq v_i(x_\alpha-) + [q_i(x_\alpha+) - q_i(x_\alpha-)].$$

These definitions trivially imply

$$q_i(x) = v_i(x) - u_i(x) \qquad \text{for all } \ x \in \mathbb{R}, \ \ i = 1, \dots, n.$$

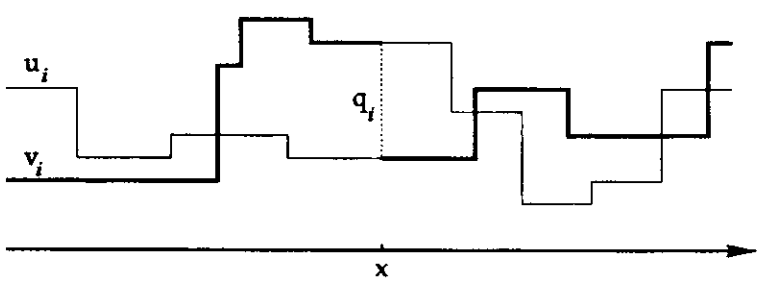

figure 23

Observe that, according to the definition (3.9), the i-waves in u and v which approach $q_i(x)$ are those located within the thick portions of the graphs of u_i, v_i in fig. 23. Viceversa, for a given i-wave σ_α located at

x_α, the regions where the jumps $q_i(x)$ approach σ_α are represented by the shaded areas in in fig. 24.

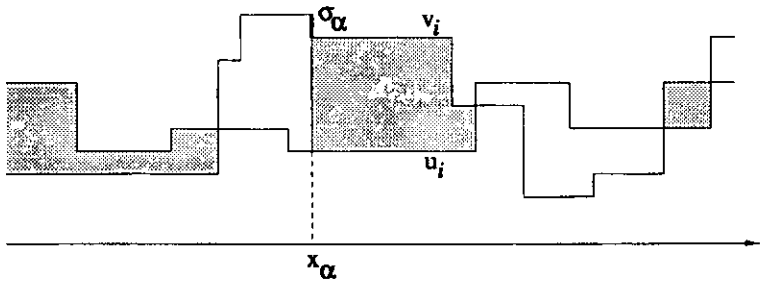

figure 24

Now let v have a wave-front at x_α with strength σ_α, in the genuinely nonlinear k-th family. To fix the ideas, assume that $v_k(x_\alpha\pm) > u_k(x_\alpha)$. In connection with this front, for every $i < k$ the functional $\Phi(u, v)$ contains a term of the form (fig. 25)

$$A_{\alpha,i} \doteq \kappa_1 \cdot |\sigma_\alpha| \cdot \quad \text{[area of the region between the graphs of } u_i \text{ and } v_i, \text{ to the right of } x_\alpha\text{]}.$$

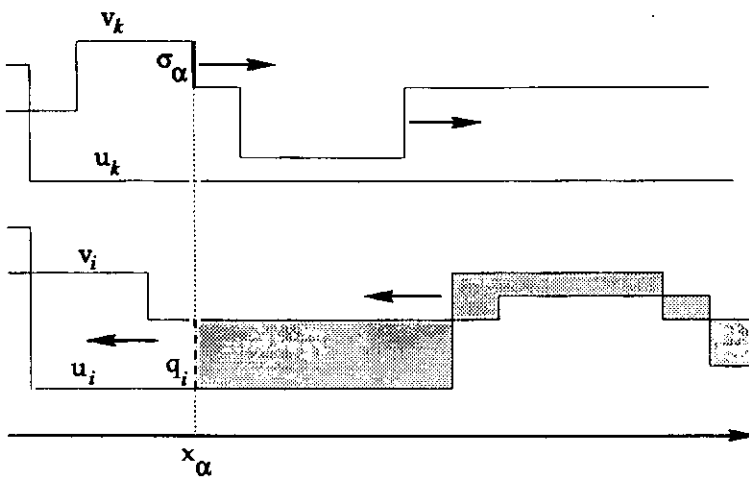

figure 25

By strict hyperbolicity, the i-th and k-th characteristic speeds are strictly separated, say $\lambda_k - \lambda_i \geq c > 0$. If each component u_i, v_i, $i =$

$1, \dots, n$, were an exact solution to a scalar conservation law:

$$(u_i)_t + F_i(u_i)_x = 0, \qquad (F_i' = \lambda_i)$$

uncoupled from all the other components, then we would have the estimate

$$\frac{dA_{\alpha,i}}{dt} \leq -\kappa_1 |\sigma_\alpha| |q_i^{\alpha+}| (\dot{x}_\alpha - \lambda_i^{\alpha+}) \leq -c\kappa_1 |\sigma_\alpha| |q_i^{\alpha+}|. \tag{3.28}$$

Here $\lambda_i^{\alpha+} \doteq \lambda_i(u_i(x_\alpha+),\ v_i(x_\alpha+))$ is a speed of an i-shock of strength $q_i^{\alpha+}$. In general, the estimate (3.28) must be supplemented with coupling and error terms, whose size is estimated as

$$\mathcal{O}(1) \cdot \left(\varepsilon + |q_k^{\alpha+}| (|q_k^{\alpha+}| + |\sigma_\alpha|) + \sum_{j \neq k} |q_j^{\alpha+}| \right) |\sigma_\alpha|. \tag{3.29}$$

A detailed computation thus yields

$$E_{\alpha,i} \leq \mathcal{O}(1) \cdot \left(\varepsilon + |q_k^{\alpha+}| (|q_k^{\alpha+}| + |\sigma_\alpha|) + \sum_{j \neq k} |q_j^{\alpha+}| \right) |\sigma_\alpha| - c\kappa_1 |q_i^{\alpha+}| |\sigma_\alpha| i \neq k. \tag{3.30}$$

Next, according to (3.9) the functional $\Phi(u, v)$ also contains a term of the form

$$A_{\alpha,k} \doteq \kappa_1 \cdot |\sigma_\alpha| \cdot \quad [\text{area of the region between the graphs of } u_k \text{ and } v_k, \text{ to the right of } x_\alpha].$$

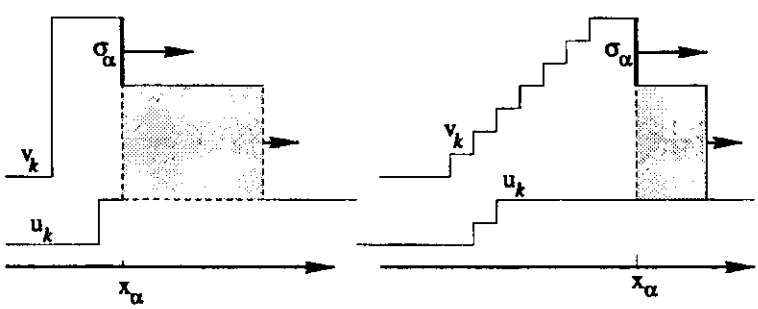

figure 26

If the components u_k, v_k were exact solutions of a genuinely nonlinear scalar conservation law, say

$$(u_k)_t + F_k(u_k)_x = 0, \qquad (F_k' = \lambda_k) \tag{3.31}$$

with $F_k'' \geq c' > 0$, then one would have the estimate

$$\frac{dA_{\alpha,k}}{dt} \leq -\kappa_1 |\sigma_\alpha| |q_k^{\alpha+}| (\dot{x}_\alpha - \lambda_k^{\alpha+}) \leq -\kappa_1 |\sigma_\alpha| |q_k^{\alpha+}| \cdot \frac{c'}{2} (|q_k^{\alpha+}| + |\sigma_\alpha|). \tag{3.32}$$

The decrease of this area is illustrated in fig. 26. In general, the estimate (3.32) must be supplemented with coupling and error terms, whose size is again estimated as (3.29). A detailed computation thus yields

$$\begin{aligned} E_{\alpha,k} \quad &\leq \mathcal{O}(1) \cdot \Big(\varepsilon + |q_k^{\alpha+}| (|q_k^{\alpha+}| + |\sigma_\alpha|) + \textstyle\sum_{j \neq k} |q_j^{\alpha+}|\Big) |\sigma_\alpha| \\ &\quad - \tfrac{c' \kappa_1}{2} |q_k^{\alpha+}| |\sigma_\alpha| (|q_k^{\alpha+}| + |\sigma_\alpha|). \end{aligned} \tag{3.33}$$

Choosing κ_1 sufficiently large, (3.30) and (3.33) together yield (3.23).

A different estimate is needed in the case where the jump in v_k crosses the graph of u_k, say $v_k(x_\alpha+) < u_k(x_\alpha) < v_k(x_\alpha-)$. To fix the ideas, assume

$$|q_k^{\alpha+}| = |v_k(x_\alpha+) - u_k(x_\alpha)| \leq |v_k(x_\alpha-) - u_k(x_\alpha)| = |q_k^{\alpha-}|. \tag{3.34}$$

In this case, the estimates (3.30) remain valid. In connection with the k-th field, the functional Φ contains a term of the form (fig. 27):

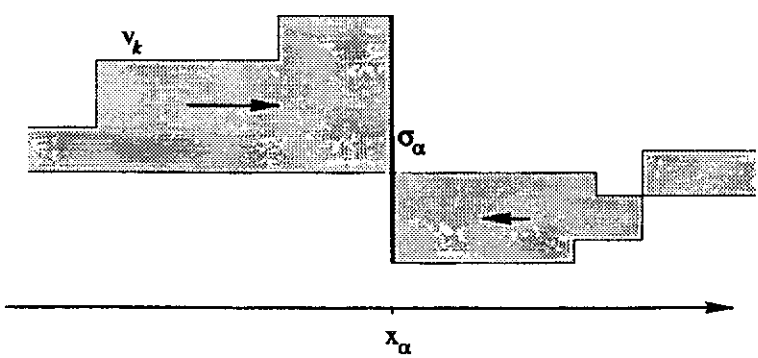

figure 27

$$A_{\alpha,k} \doteq [\text{area of the region between the graphs of } u_k \text{ and } v_k|, \quad (3.35)$$

where the above area includes points both to the right and to the left of x_α.

If the components u_k, v_k provided an exact solution to the genuinely nonlinear scalar conservation law (3.31), due to genuine nonlinearity we would have

$$\frac{dA_{\alpha,k}}{dt} \leq -\frac{c'}{2}|q_k^{\alpha-}| \cdot |q_k^{\alpha+}| \leq -\frac{c'}{4}|\sigma_\alpha||q_k^{\alpha+}|. \quad (3.36)$$

Indeed, by (3.34),

$$|\sigma_\alpha| = |q_k^{\alpha-}| + |q_k^{\alpha+}| \leq 2|q_k^{\alpha-}|.$$

In general, the estimate (3.36) must be supplemented with coupling and error terms, whose size is again estimated as (3.29). A detailed computation thus yields

$$E_{\alpha,k} \leq \mathcal{O}(1) \cdot \left(\varepsilon + |q_k^{\alpha+}|(|q_k^{\alpha+}| + |\sigma_\alpha|) + \sum_{j \neq k} |q_j^{\alpha+}|\right) |\sigma_\alpha| - \frac{c'}{4}|q_k^{\alpha+}||\sigma_\alpha|. \quad (3.37)$$

Assuming that the total strength of waves remains sufficiently small, we have

$$|q_k^{\alpha+}| + |\sigma_\alpha| \ll \frac{c'}{4},$$

hence (3.30) and (3.37) together yield (3.23). For details we again refer to [11].

4 Uniqueness of solutions

Having proved that the limits of front tracking approximations are unique and determine a semigroup of solutions, we would like to show that this semigroup is canonically associated with the system (2.1). In other words, when $\bar{u} \in \mathcal{D}$, the semigroup trajectory $t \mapsto S_t\bar{u}$ is the unique entropy weak solution to the corresponding Cauchy problem. For scalar conservation laws, a very general uniqueness and stability result was

proved in the fundamental paper of Kruzhkov [17]. In the case of $n \times n$ systems, under some mild regularity assumptions, results in this direction were recently obtained in [8, 9, 10]. For sake of clarity, a complete set of assumptions is listed below.

(A1) **(Conservation Equations)** The function $u = u(t,x)$ is a weak solution of the Cauchy problem (2.1)-(2.2), taking values within the domain $\mathcal{D}$ of a semigroup S. More precisely, $u : [0,T] \mapsto \mathcal{D}$ is continuous w.r.t. the $\mathbf{L}^1$ distance. The initial condition (2.2) holds, together with

$$\iint (u\varphi_t + f(u)\varphi_x)\, dxdt = 0 \tag{4.1}$$

for every $\mathcal{C}^1$ function φ with compact support contained inside the open strip $]0,T[\times \mathbb{R}$.

(A2) **(Entropy Condition)** Let u have an approximate jump discontinuity at some point $(\tau,\xi) \in]0,T[\times\mathbb{R}$. More precisely, let there exists states $u^-, u^+ \in \Omega$ and a speed $\lambda \in \mathbb{R}$ such that, calling

$$U(t,x) \doteq \begin{cases} u^- & \text{if } x < \xi + \lambda(t-\tau), \\ u^+ & \text{if } x > \xi + \lambda(t-\tau), \end{cases} \tag{4.2}$$

there holds

$$\lim_{\rho \to 0+} \frac{1}{\rho^2} \int_{\tau-\rho}^{\tau+\rho} \int_{\xi-\rho}^{\xi+\rho} \Big| u(t,x) - U(t,x) \Big|\, dxdt = 0. \tag{4.3}$$

Then, for some $i \in \{1,\ldots,n\}$, one has the entropy inequality:

$$\lambda_i(u^-) \geq \lambda \geq \lambda_i(u^+). \tag{4.4}$$

(A3) **(Tame Oscillation Condition)** For some constants C, $\hat{\lambda}$ the following holds. For every point $x \in \mathbb{R}$ and every $t, h > 0$ one has

$$|u(t+h,x) - u(t,x)| \leq C \cdot \text{Tot.Var.}\{u(t,\cdot); [x - \hat{\lambda}h,\ x + \hat{\lambda}h]\}. \tag{4.5}$$

(A4) **(Bounded Variation Condition)** There exists $\delta > 0$ such that, for every space-like curve $\{t = \tau(x)\}$ with $|d\tau/dx| < \delta$ a.e., the function $x \mapsto u(\tau(x),x)$ has locally bounded variation.

Remarks. Assumption (A2) generalizes the Lax entropy condition. Indeed, if (4.2)-(4.3) hold, using (4.1) one can prove that the states u^-, u^+ and the speed λ must satisfy the Rankine-Hugoniot conditions. By (1.18), the speed of the jump coincides with an eigenvalue of the averaged matrix $A(u^-, u^+)$, say $\lambda = \lambda_i(u^-, u^+)$. In this setting, the condition (4.4) requires that the speed of an i-shock be greater than the i-speed of the state u^+ ahead of the shock, but smaller than the i-speed of the state u^- behind the shock. In the t-x plane, the i-characteristic lines thus flow into the shock curve from both sides.

The condition (A3) restricts the oscillation of the solution. An equivalent, more intuitive formulation is the following. For some constant $\hat{\lambda}$ larger than all characteristic speeds, given any interval $[a, b]$ and $t \geq 0$, the oscillation of u on the triangle $\Delta \doteq \{(s, y) : \ s \geq t, \ a + \hat{\lambda} s < y < b - \hat{\lambda} s\}$, defined as

$$\mathrm{Osc}\{u; \ \Delta\} \doteq \sup_{(s,y),(s',y') \in \Delta} |u(s, y) - u(s', y')|,$$

is bounded by a constant multiple of the total variation of $u(t, \cdot)$ on $[a, b]$. Assumption (A4) simply requires that, for some fixed $\delta > 0$, the function u has bounded variation along all space-like curves $\{t = \tau(x); \ x \in [a, b]\}$ with slope $\leq \delta_\perp$ i.e. with

$$|\tau(x) - \tau(x')| \leq \delta |x - x'| \qquad \text{for all } \ x, x' \in [a, b].$$

One can prove that all of the above assumptions are satisfied by weak solutions obtained as limits of Glimm or wave-front tracking approximations. The following result shows that the entropy weak solution of the Cauchy problem (2.1)-(2.2) is unique within the class of functions that satisfy either the additional regularity condition (A3), or (A4).

Theorem 5. *Let the map $u : [0, T] \mapsto \mathcal{D}$ be continuous (w.r.t. the $\mathbf{L}^1$ distance), taking values in the domain of the semigroup S generated by the system (2.1). If* (A1), (A2) *and* (A3) *hold, then*

$$u(t, \cdot) = S_t \bar{u} \qquad \textit{for all } \ t \in [0, T]. \tag{4.6}$$

In particular, the weak solution that satisfies these conditions is unique. The same conclusion holds if the assumption (A3) *is replaced by* (A4).

The first part of Theorem 5 follows from the results in [8], the second part was proved in [10]. The main steps of the proof are given below.

1. Since u takes values inside the domain $\mathcal{D}$ of the semigroup, the total variation of $u(t,\cdot)$ remains uniformly bounded. From the basic equation (2.1), it follows that u is Lipschitz continuous with values in $\mathbf{L}^1$, namely

$$\|u(t)-u(s)\|_{\mathbf{L}^1} \leq L\cdot|t-s| \tag{4.7}$$

for some Lipschitz constant L. More precisely, if M and λ^* are constants such that

$$\text{Tot.Var.}(u)\leq M \qquad \text{for all } u\in\mathcal{D},$$

$$|f(\omega)-f(\omega')|\leq\lambda^*|\omega-\omega'| \qquad \text{whenever } |\omega|,|\omega'|\leq M,$$

as Lipschitz constant in (4.7) one can take $L\doteq\lambda^*M$. As a consequence, $u=u(t,x)$ can be regarded as a BV function of the two variables t,x, in the sense that the distributional derivatives D_tu, D_xu are Radon measures. By a well known structure theorem [14], there exists a set $\widetilde{\mathcal{N}}\subset]0,T[\times\mathbb{R}$ of 1-dimensional Hausdorff measure zero such that, at every point $(\tau,\xi)\notin\widetilde{\mathcal{N}}$, u either is approximately continuous or has an approximate jump discontinuity. Taking the projection of $\widetilde{\mathcal{N}}$ on the t-axis, we conclude that there exists a set $\mathcal{N}\subset[0,T]$ of measure zero, containing the endpoints 0 and T, such that, at every point $(\tau,\xi)\in[0,T]\times\mathbb{R}$ with $\tau\notin\mathcal{N}$, setting $u^-\doteq u(\tau,\xi-)$, $u^+\doteq u(\tau,\xi+)$ the following property holds.

(P) Either $u^+=u^-$, in which case (4.2)-(4.3) hold with λ arbitrary. Or else $u^+\neq u^-$, in which case (4.2)-(4.3) hold for some particular $\lambda\in\mathbb{R}$. In this second case, for some $i\in\{1,\ldots,n\}$ the Rankine-Hugoniot equations and the Lax entropy condition hold:

$$\begin{aligned}\lambda_i(u^-,u^+)\cdot(u^+-u^-) &= f(u^+)-f(u^-),\\ \lambda_i(u^-) &\geq \lambda_i(u^-,u^+)\geq\lambda_i(u^+).\end{aligned}\tag{4.8}$$

2. The identity (4.6) will be proved by means of the error estimate:

$$\|u(T)-S_Tu(0)\|_{\mathbf{L}^1}\leq L\cdot\int_0^T\left\{\liminf_{h\to0+}\frac{\|u(t+h)-S_hu(t)\|_{\mathbf{L}^1}}{h}\right\}dt, \tag{4.9}$$

valid for every Lipschitz continuous map $u : [0, T] \mapsto \mathcal{D}$. Observe that the integrand in (4.9) can be interpreted as an *instantaneous error rate.* As shown in fig. 28, the distance $\|u(T) - S_T u(0)\|_{\mathbf{L}^1}$ is bounded by the length of the path $t \mapsto S_{T-t} u(t)$. In turn, this length is obtained by integrating the instantaneous error rate, magnified by a factor L. Indeed

$$\|S_{T-(t+h)} u(t+h) - S_{T-t} u(t)\| \leq L \cdot \|u(t+h) - S_h u(t)\|.$$

For a detailed proof of (4.8), see [4, 5].

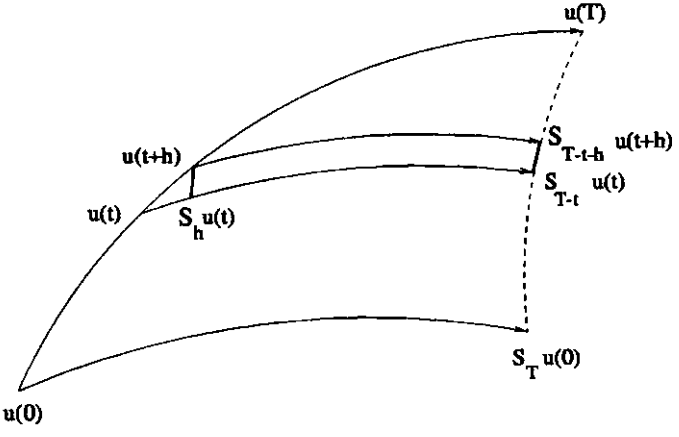

figure 28

We will establish (4.6) by showing that the integrand on the right hand side of (4.9) vanishes at each time $t \notin \mathcal{N}$. Because of the finite speed of propagation, it actually suffices to show that, for each $t \notin \mathcal{N}$, $\varepsilon > 0$ and every interval $[a, b]$, there holds

$$\limsup_{h \to 0+} \frac{1}{h} \int_a^b \Big| u(t+h,\ x) - (S_h u(t))(x) \Big|\, dx = \mathcal{O}(1) \cdot \varepsilon. \tag{4.10}$$

3. Let $u = u(t, x)$ be as in Theorem 5. In the following, for any given point (τ, ξ), we denote by $U^\sharp = U^\sharp_{(\tau,\xi)}$ the solution of the Riemann problem

$$w_t + f(w)_x = 0,\ w(\tau, x) = \begin{cases} u^+ \doteq u(\tau, \xi+) & \text{if} \quad x > \xi, \\ u^- \doteq u(\tau, \xi-) & \text{if} \quad x < \xi. \end{cases} \tag{4.11}$$

By the property (P), apart from the trivial case where $u^+ = u^-$, this solution consists of a single entropy admissible shock. The function $U^\sharp$ provides a good approximation to the solution u in a forward neighborhood of the point (τ, ξ). More precisely, using the Lipschitz continuity (4.7), one can prove that

$$\lim_{h\to 0+} \frac{1}{h} \int_{\xi - h\hat\lambda}^{\xi + h\hat\lambda} \Big| u(\tau + h,\ x) - U^\sharp_{(\tau,\xi)}(\tau + h,\ x) \Big|\ dx = 0, \tag{4.12}$$

for every $\hat\lambda > 0$ and every (τ, ξ) with $\tau \notin \mathcal{N}$.

4. Next, for a given point (τ, ξ) we denote by $U^\flat = U^\flat_{(\tau,\xi)}$ the solution of the linear system with constant coefficients

$$w_t + \widetilde{A} w_x = 0, \qquad\qquad w(\tau, x) = u(\tau, x), \tag{4.13}$$

where $\widetilde{A} \doteq A(u(\tau, \xi))$. As in the previous step, we need to estimate the difference between u and $U^\flat$, in a forward neighborhood of the point (τ, ξ). Consider any open interval $]a, b[$ containing the point ξ and fix a speed $\hat\lambda$ strictly larger than the absolute values of all characteristic speeds. For $t \geq \tau$ define the open intervals

$$J(t) \doteq\ ]a + (t - \tau)\hat\lambda,\ \ b - (t - \tau)\hat\lambda[\tag{4.14}$$

and the region

$$\Gamma(t) \doteq \{(s, x);\quad s \in [\tau,\ t],\ \ x \in J(s)\}. \tag{4.15}$$

With the above notation we claim that, for every $\tau' \geq \tau$,

$$\begin{aligned} \int_{J(\tau')} \Big| u(\tau',\ x) - U^\flat(\tau',\ x) \Big|\ dx &= \mathcal{O}(1) \cdot \sup_{(t,x)\in\Gamma(\tau')} |u(t, x) - u(\tau, \xi)| \\ &\cdot \int_\tau^{\tau'} \text{Tot.Var.}\{u(t, \cdot);\ J(t)\}\ dt. \end{aligned} \tag{4.16}$$

To derive (4.16), call $\tilde\lambda_i$, $\tilde l_i$, $\tilde r_i$ respectively the i-th eigenvalues and left and right eigenvectors of the matrix $\widetilde{A}$. Solving (4.13) we find

$$\tilde l_i \cdot U^\flat(\tau', x) = \tilde l_i \cdot U^\flat(\tau, x - (\tau' - \tau)\tilde\lambda_i) = \tilde l_i \cdot u(\tau, x - (\tau' - \tau)\tilde\lambda_i).$$

Now fix any $\zeta', \zeta'' \in J(\tau')$ and consider the quantity

$$\begin{aligned} E_i(\zeta', \zeta'') &\doteq \tilde{l}_i \cdot \int_{\zeta'}^{\zeta''} (u(\tau', x) - U^\flat(\tau', x))\, dx \\ &= \tilde{l}_i \cdot \int_{\zeta'}^{\zeta''} \Big(u(\tau', x) - u(\tau,\ x - (\tau' - \tau)\tilde{\lambda}_i)\Big)\, dx. \end{aligned} \tag{4.17}$$

Since u satisfies the conservation equation (2.1) over the domain

$$D_i \doteq \Big\{(t, x);\ \ t \in [\tau,\ \tau'],\ \ \zeta' + (t - \tau')\tilde{\lambda}_i \le x \le \zeta'' + (t - \tau')\tilde{\lambda}_i\Big\},$$

the difference between the integral of u at the top and at the bottom of the domain D_i is measured by the inflow from the left side minus the outflow from the right side (fig. 29).

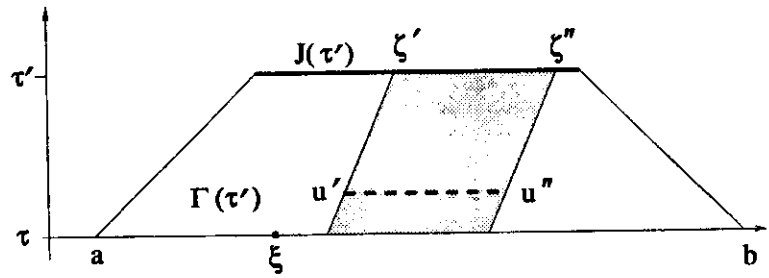

figure 29

From (4.17) it thus follows

$$\begin{aligned} E_i = \ & \int_\tau^{\tau'} \tilde{l}_i \cdot \Big((f(u) - \tilde{\lambda}_i u)(t,\ \zeta' + (t - \tau')\tilde{\lambda}_i)\Big)\, dt \\ & - \int_\tau^{\tau'} \tilde{l}_i \cdot \Big((f(u) - \tilde{\lambda}_i u)(t,\ \zeta'' + (t - \tau')\tilde{\lambda}_i)\Big)\, dt. \end{aligned} \tag{4.18}$$

To estimate the quantity in (4.18), consider the states

$$u'(t) \doteq u(t,\ \zeta' + (t - \tau')\tilde{\lambda}_i),\ u''(t) \doteq u(t,\ \zeta'' + (t - \tau')\tilde{\lambda}_i),\ \tilde{u} \doteq u(\tau, \xi).$$

We then have

$$\tilde{l}_i \cdot [f(u'') - f(u') - \tilde{\lambda}_i(u'' - u')] = \tilde{l}_i \cdot [Df(\tilde{u}) \cdot (u'' - u') - \tilde{\lambda}_i(u'' - u')] + \tilde{l}_i \cdot A^* \cdot (u'' - u'), \tag{4.19}$$

where A^* is the averaged matrix

$$A^* \doteq \int_0^1 \Big[Df(su'' + (1 - s)u') - Df(\tilde{u})\Big]\, ds.$$

Since the first term on the right hand side of (4.19) vanishes, we thus obtain

$$\begin{aligned}&\Big|\tilde{l}_i\cdot\big(f(u'')-f(u')-\tilde{\lambda}_i(u''-u')\big)\Big|\\&=\ \mathcal{O}(1)\cdot|u''-u'|\cdot(|u''-\tilde{u}|+|u'-\tilde{u}|),\\&=\mathcal{O}(1)\cdot\text{Tot.Var.}\Big\{u(t);\ [\zeta'+(t-\tau')\tilde{\lambda}_i,\ \zeta''+(t-\tau')\tilde{\lambda}_i]\Big\}\\&\cdot\sup_{(t,x)\in\Gamma(\tau')}|u(t,x)-u(\tau,\xi)|.\end{aligned}\tag{4.20}$$

In turn, (4.20) yields

$$\begin{aligned}|E_i(\zeta',\zeta'')|&=\mathcal{O}(1)\cdot\sup_{(t,x)\in\Gamma(\tau')}|u(t,x)-u(\tau,\xi)|\\&\cdot\int_\tau^{\tau'}\text{Tot.Var.}\Big\{u(t,\cdot);\ [\zeta'+(t-\tau')\tilde{\lambda}_i,\ \zeta''+(t-\tau')\tilde{\lambda}_i]\Big\}\,dt.\end{aligned}\tag{4.21}$$

Since the estimate (4.21) holds for all $i=1,\dots,n$ and all $\zeta',\zeta''\in J(\tau')$, it implies (4.16).

5. Given $\tau\notin\mathcal{N}$, $\varepsilon>0$ and $a<b$, using either one of the assumptions (A3) or (A4) we can cover a neighborhood of the interval $[a,b]$ with finitely many points ξ_i and open intervals $I_j\doteq]a_j,\ b_j[$ such that the following conditions hold (fig. 30).

(i) Each point x is contained in at most two of the open intervals I_j.

(ii) The total variation of $u(\tau,\cdot)$ on each I_j is $\leq\varepsilon$.

(iii) For some $\tau'>\tau$, calling $\zeta_j\doteq(a_j+b_j)/2$ and

$$\Gamma_j\doteq\Big\{(t,x);\quad t\in[\tau,\tau'],\ \ a_j+(t-\tau)\hat{\lambda}\ <\ x\ <\ b_j-(t-\tau)\hat{\lambda}[\Big\},$$

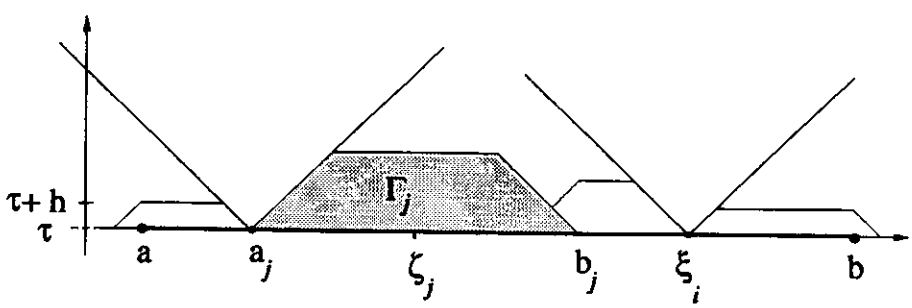

figure 30

there holds

$$\sup_{(t,x)\in\Gamma_j}|u(t,x)-u(\tau,\zeta_j)|\leq\varepsilon.\tag{4.22}$$

6. We now construct a function $U = U(t,x)$ which coincides with $U^{\sharp}_{(\tau,\xi_i)}$ near each point (τ,ξ_i) and with $U^{\flat}_{(\tau,\zeta_j)}$ in a forward neighborhood of each point (τ,ζ_j).

$$U(t,x) \doteq \begin{cases} U^{\sharp}_{(\tau,\xi_i)}(t,x) & \text{if} \quad |x-\xi_i| \leq (t-\tau)\hat{\lambda}, \\ U^{\flat}_{(\tau,\zeta_j)}(t,x) & \text{if} \quad (t,x) \in \Gamma_j \setminus \bigcup_{k<j} \Gamma_k. \end{cases}$$

By (4.12) and (4.16), this function U provides a good approximation of u, for times $t = \tau + h$ with $h > 0$ small. Indeed, recalling (4.22) and the property (i) of the covering, we have

$$\begin{aligned} \limsup_{h\to 0+} \quad & \frac{1}{h}\int_a^b \Big|u(\tau+h,\ x) - U(\tau+h,\ x)\Big|\ dx \\ & \leq \sum_i \limsup_{h\to 0+} \frac{1}{h}\int_{\xi_i - h\hat{\lambda}}^{\xi_i + h\hat{\lambda}} \Big|u(\tau+h,\ x) - U^{\sharp}_{(\tau,\xi_i)}(\tau+h,\ x)\Big|\ dx \\ & + \sum_j \limsup_{h\to 0+} \frac{1}{h}\int_{a_j + h\hat{\lambda}}^{b_j - h\hat{\lambda}} \Big|u(\tau+h,\ x) - U^{\flat}_{(\tau,\zeta_j)}(\tau+h,\ x)\Big|\ dx \\ & \leq 0 + \limsup_{h\to 0+} \left\{ \mathcal{O}(1)\cdot \sum_j \frac{\varepsilon}{h}\int_\tau^{\tau+h} \text{Tot.Var.}\{u(t);\ \ I_j\}\ dt \right\} \\ & \leq \limsup_{h\to 0+} \left\{ \mathcal{O}(1)\cdot \frac{\varepsilon}{h}\int_\tau^{\tau+h} 2\cdot \text{Tot.Var.}\{u(t);\ \ \mathbb{R}\}\ dt \right\} \\ & = \mathcal{O}(1)\cdot\varepsilon. \end{aligned} \tag{4.23}$$

7. We now observe that the semigroup trajectory $v(t,\cdot) \doteq S_t\bar{u}$ is also an entropy weak solution to the Cauchy problem (2.1)-(2.2), and satisfies all the assumptions (A1)–(A3). In particular, the total variation of $v(t,\cdot)$ remains uniformly bounded, and its oscillation on each domain $\Gamma(t)$ of the form (4.15) is bounded by

$$\sup_{(t,x)\in\Gamma(\tau')} |v(t,x) - v(\tau,\xi)| = \mathcal{O}(1)\cdot \text{Tot.Var.}\{v(\tau);\ \ ]a,b[\,\}. \tag{4.24}$$

As a consequence, we can repeat the estimate (4.23) with v in the role of u and obtain

$$\limsup_{h\to 0+} \frac{1}{h}\int_a^b \Big|v(\tau+h,\ x) - U(\tau+h,\ x)\Big|\ dx = \mathcal{O}(1)\cdot\varepsilon. \tag{4.25}$$

Together, (4.23) and (4.25) imply (4.10). Since $\varepsilon > 0$ and the interval $[a, b]$ were arbitrary, this achieves the proof of Theorem 5.

Aknowledgment. The present work was supported by the European TMR Contract ERB FMRX CT96 0033 on Hyperbolic Systems of Conservation Laws.

References

[1] P. Baiti and H. K. Jenssen, On the front tracking algorithm, *J. Math. Anal. Appl.* **217** (1998), 395-404.

[2] A.Bressan, Contractive metrics for nonlinear hyperbolic systems, *Indiana Univ. Math. J.* **37** (1988), 409-421.

[3] A. Bressan, Global solutions of systems of conservation laws by wave-front tracking, *J. Math. Anal. Appl.* **170** (1992), 414-432.

[4] A. Bressan, The unique limit of the Glimm scheme, *Arch. Rational Mech. Anal.* **130** (1995), 205-230.

[5] A. Bressan, On the Cauchy problem for nonlinear hyperbolic systems, Proceedings CANum'97, C. Carasso Ed., http://www.emath.fr/Maths/Proc/proc.html

[6] A. Bressan and R. M. Colombo, The semigroup generated by 2×2 conservation laws, *Arch. Rational Mech. Anal.* **133** (1995), 1-75.

[7] A. Bressan, G. Crasta, and B. Piccoli, Well posedness of the Cauchy problem for $n \times n$ systems of conservation laws, Amer. Math. Soc. Memoir, to appear.

[8] A. Bressan and P. Goatin, Oleinik type estimates and uniqueness for $n \times n$ conservation laws, *J. Differential Equations*, to appear.

[9] A. Bressan and P. LeFloch, Uniqueness of weak solutions to hyperbolic systems of conservation laws. *Arch. Rational Mech. Anal.* **140** (1997), 301-317.

[10] A. Bressan and M. Lewicka, A uniqueness condition for hyperbolic systems of conservation laws, Preprint S.I.S.S.A., Trieste 1998.

[11] A. Bressan, T. P. Liu and T. Yang, L^1 stability estimates for $n \times n$ conservation laws, *Arch. Rational Mech. Anal.*, to appear.

[12] C. Dafermos, Polygonal approximations of solutions of the initial value problem for a conservation law, *J. Math. Anal. Appl.* **38** (1972), 33-41.

[13] R. J. DiPerna, Global existence of solutions to nonlinear hyperbolic systems of conservation laws, *J. Differential Equations* **20** (1976), 187-212.

[14] L. C. Evans and R. F. Gariepy, *Measure Theory and Fine Properties of Functions*, C.R.C. Press, 1992.

[15] J. Glimm, Solutions in the large for nonlinear hyperbolic systems of equations, *Comm. Pure Appl. Math.* **18** (1965), 697-715.

[16] F. John, Formation of singularities in one-dimensional nonlinear wave propagation, *Comm. Pure Appl. Math.* **27** (1974), 377-405.

[17] S. Kruzhkov, First-order quasilinear equations with several space variables, *Mat. Sb.* **123** (1970), 228–255. English transl. in *Math. USSR Sb.* **10** (1970), 217–273.

[18] P. D. Lax, Hyperbolic systems of conservation laws II, *Comm. Pure Appl. Math.* **10** (1957), 537-566.

[19] T.-P. Liu and T. Yang, L^1 stability of conservation laws with coinciding Hugoniot and characteristic curves, *Indiana Univ. Math. J.*, to appear.

[20] T.-P. Liu and T. Yang, L^1 stability of weak solutions for 2×2 systems of hyperbolic conservation laws, *J. Amer. Math. Soc.*, to appear.

[21] N. H. Risebro, A front-tracking alternative to the random choice method, *Proc. Amer. Math. Soc.* **117** (1993), 1125-1139.

[22] B. L. Rozdesvenskii and N. Yanenko, *Systems of Quasilinear Equations and Their Applications to Gas Dynamics*, A.M.S. Translations of Mathematical Monographs **55**, Providence, 1983.

[23] D. Serre, *Systemes de Lois de Conservation*, Diderot Editeur, 1996.

[24] J. Smoller, *Shock Waves and Reaction-Diffusion Equations*, Springer-Verlag, New York, 1983.

[25] B. Temple, Systems of conservation laws with invariant submanifolds, *Trans. Amer. Math. Soc.* **280** (1983), 781-795.

Sector of Functional Analysis
International School for Advances Studies
Trieste, ITALY
e-mail: bressan@sissa.it

Recibido: 28 de Octubre de 1998